

1 **Expanding the diversity of bacterioplankton isolates and modeling isolation efficacy with**
2 **large scale dilution-to-extinction cultivation**

3
4
5
6
7
8
9
10
11
12
13
14
15
16
17
18
19
20
21
22
23
24
25
26
27
28
29
30
31
32
33
34
35
36
37
38
39
40
41
42
43
44
45
46

Michael W. Henson^{1,#}, V. Celeste Lanclos¹, David M. Pitre², Jessica Lee Weckhorst^{2,†}, Anna M. Lucchesi², Chuankai Cheng¹, Ben Temperton^{3*}, and J. Cameron Thrash^{1*}

¹Department of Biological Sciences, University of Southern California, Los Angeles, CA 90089, U.S.A.

²Department of Biological Sciences, Louisiana State University, Baton Rouge, LA 70803, U.S.A.

³School of Biosciences, University of Exeter, Stocker Road, Exeter, EX4 4QD, U.K.

[#]Current affiliation: Department of Geophysical Sciences, University of Chicago, Chicago, IL 60637, U.S.A.

[†]Quantitative and Computational Biosciences Program, Baylor College of Medicine, Houston, TX 77030, U.S.A.

*Correspondence:

J. Cameron Thrash
thrash@usc.edu

Ben Temperton
b.temperton@exeter.ac.uk

Running title: Evaluation of large-scale DTE cultivation

Keywords: dilution-to-extinction, cultivation, bacterioplankton, LSUCC, microbial ecology, coastal microbiology

47
48
49
50
51
52
53
54
55
56
57
58
59
60
61
62
63
64
65
66
67
68
69
70
71
72
73
74
75
76
77
78
79
80
81
82
83
84
85
86
87
88
89
90
91
92

Abstract

Cultivated bacterioplankton representatives from diverse lineages and locations are essential for microbiology, but the large majority of taxa either remain uncultivated or lack isolates from diverse geographic locales. We paired large scale dilution-to-extinction (DTE) cultivation with microbial community analysis and modeling to expand the phylogenetic and geographic diversity of cultivated bacterioplankton and to evaluate DTE cultivation success. Here, we report results from 17 DTE experiments totaling 7,820 individual incubations over three years, yielding 328 repeatably transferable isolates. Comparison of isolates to microbial community data of source waters indicated that we successfully isolated 5% of the observed bacterioplankton community throughout the study. 43% and 26% of our isolates matched operational taxonomic units (OTUs) and amplicon single nucleotide variants (ASVs), respectively, within the top 50 most abundant taxa. Isolates included those from previously uncultivated clades such as SAR11 LD12 and *Actinobacteria* acIV, as well as geographically novel members from other ecologically important groups like SAR11 subclade IIIa, SAR116, and others; providing the first isolates in eight genera and seven species. Using a newly developed DTE cultivation model, we evaluated taxon viability by comparing relative abundance with cultivation success. The model i) revealed the minimum attempts required for successful isolation of taxa amenable to growth on our media, and ii) identified important and abundant taxa such as SAR11 with low viability that likely impacts cultivation success. By incorporating viability in experimental design, we can now statistically constrain the number of attempts necessary for successful cultivation of a given taxon on a defined medium.

Importance

Even before the coining of the term “great plate count anomaly” in the 1980s, scientists had noted the discrepancy between the number of microorganisms observed under the microscope and the number of colonies that grew on traditional agar media. New cultivation approaches have reduced this disparity, resulting in the isolation of some of the “most wanted” bacterial lineages. Nevertheless, the vast majority of microorganisms remain uncultured, hampering progress towards answering fundamental biological questions about many important microorganisms. Furthermore, few studies have evaluated the underlying factors influencing cultivation success, limiting our ability to improve cultivation efficacy. Our work details the use of dilution-to-extinction (DTE) cultivation to expand the phylogenetic and geographic diversity of available axenic cultures. We also provide a new model of the DTE approach that uses cultivation results and natural abundance information to predict taxon-specific viability and iteratively constrain DTE experimental design to improve cultivation success.

93 Introduction

94 Axenic cultures of environmentally important microorganisms are critical for
95 fundamental microbiological investigation, including generating physiological information about
96 environmental tolerances, determining organismal-specific metabolic and growth rates, testing
97 hypotheses generated from *in situ* 'omics observations, and experimentally examining microbial
98 interactions. Research using important microbial isolates has been critical to a number of
99 discoveries such as defining microorganisms involved in surface ocean methane saturation (1–3),
100 the role of proteorhodopsin in maintaining cellular functions during states of carbon starvation
101 (4, 5), the complete nitrification of ammonia within a single organism (6), and identifying novel
102 metabolites and antibiotics (7–10). However, the vast majority of taxa remain uncultivated (11–
103 13), restricting valuable experimentation on such topics as genes of unknown function, the role
104 of analogous gene substitutions in overcoming auxotrophy, and the multifaceted interactions
105 occurring in the environment inferred from sequence data (11, 14–16).

106 The quest to bring new microorganisms into culture, and the recognition that traditional
107 agar-plate based approaches have limited success (17–19), have compelled numerous
108 methodological advances spanning a wide variety of techniques like diffusion chambers,
109 microdroplet encapsulation, and slow acclimatization of cells to artificial media (20–25).
110 Dilution-to-extinction (DTE) cultivation using sterile seawater as the medium has also proven
111 highly successful for isolating bacterioplankton (26–32). Pioneered by Don Button and
112 colleagues for the cultivation of oligotrophic bacteria, this method essentially pre-isolates
113 organisms after serial dilution by separating individual or small groups of cells into their own
114 incubation vessel (32, 33). This prevents slow-growing, obligately oligotrophic bacterioplankton
115 from being outcompeted by faster-growing organisms, as would occur in enrichment-based
116 isolation methods, particularly those that would target aerobic heterotrophs. It is also a practical
117 method for taxa that cannot grow on solid media. Natural seawater media provide these taxa with
118 the same chemical surroundings from which they are collected, reducing the burden of
119 anticipating all the relevant compounds required for growth (33).

120 Improvements to DTE cultivation in multiple labs have increased the number of
121 inoculated wells and decreased the time needed to detect growth (26, 28, 34), thereby earning the
122 moniker “high-throughput culturing” (26, 28). We (35) and others (30) have also adapted DTE
123 culturing by incorporating artificial media in place of natural seawater media to successfully
124 isolate abundant bacterioplankton. Thus far, DTE culturing has led to isolation of many
125 numerically abundant marine and freshwater groups such as marine SAR11 Alphaproteobacteria
126 (28, 29, 34–36), the freshwater SAR11 LD12 clade (29), SUP05/Arctic96BD-19
127 *Gammaproteobacteria* (37–39), OM43 *Betaproteobacteria* (26, 27, 31, 40, 41), HIMB11-Type
128 *Roseobacter* (35, 42), numerous so-called Oligotrophic Marine *Gammaproteobacteria* (43), and
129 *actI Actinobacteria* (44).

130 Despite the success of DTE cultivation, many taxa continue to elude domestication (11–
131 13, 16). Explanations include a lack of required nutrients or growth factors in media (20, 45–49)
132 and biological phenomena such as dormancy and/or phenotypic heterogeneity within populations
133 (47, 48, 50–56). However, there have been few studies empirically examining the factors
134 underlying isolation success in DTE cultivation experiments (34, 57, 58), restricting our ability
135 to determine the relative importance of methodological vs. biological influences on cultivation
136 reliability for any given organism. Moreover, even for those taxa that we have successfully
137 cultivated, in many cases we lack geographically diverse strains, restricting comparisons of the
138 phenotypic and genomic diversity that may influence taxon-specific cultivability.

139 We undertook a three-year cultivation effort in the coastal northern Gulf of Mexico
140 (nGOM), from which we lack representatives of many common bacterioplankton groups, to
141 provide new model organisms for investigating microbial function, ecology, biogeography, and
142 evolution. Simultaneously, we paired our cultivation efforts with 16S rRNA gene amplicon
143 analyses to compare cultivation results with the microbial communities in the source waters. We
144 have previously reported on the success of our artificial media in obtaining abundant taxa over
145 the course of seven experiments from this campaign (35). Here, we expand our report to include
146 the cultivation results from a total of seventeen experiments, and update the classic viability
147 calculations of Button *et al.* (33) with a new model to estimate the viability of individual taxa
148 using relative abundance information. Individuals from eight and seven cultivated groups
149 belonged to putatively novel genera and species, respectively, and our isolates expand the
150 geographic representation for many important clades like SAR11. Additionally, using model-
151 based predictions, we identify possible taxon-specific viability variation that can influence
152 cultivation success. By incorporating these new viability estimates into the model, our method
153 facilitates statistically-informed experimental design for targeting individual taxa, thereby
154 reducing uncertainty for future culturing work (59).

155

156 **Material and Methods**

157

158 *Sampling*

159 Surface water samples were collected at six different sites once a year for three years, except for
160 Terrebonne Bay, which was collected twice. The sites sampled were Lake Borgne (LKB; Shell
161 Beach, LA), Bay Pomme d'Or (JLB; Buras, LA), Terrebonne Bay (TBON; Cocodrie, LA),
162 Atchafalaya River Delta (ARD; Franklin, LA), Freshwater City (FWC; Kaplan, LA), and
163 Calcasieu Jetties (CJ; Cameron, LA) (lat/long coordinates provided in Table S1). Water
164 collection for biogeochemical and biological analysis followed the protocol in (35). Briefly, we
165 collected surface water in a sterile, acid-washed polycarbonate bottle. Duplicate 120 ml water
166 samples were filtered serially through 2.7 μm Whatman GF/D (GE Healthcare, Little Chalfort,
167 UK) and 0.22 μm Sterivex (Millipore, Massachusetts, USA) filters and placed on ice until
168 transferred to -20°C in the laboratory (maximum 3 hours on ice). The University of Washington
169 Marine Chemistry Laboratory analyzed duplicate subsamples of 50 ml 0.22 μm -filtered water
170 collected in sterile 50 ml falcon tubes (VWR, Pennsylvania, USA) for concentrations of SiO_4 ,
171 PO_4^{3-} , NH_4^+ , NO_3^- , and NO_2^- . Samples for cell counts were filtered through a 2.7 μm GF/D filter,
172 fixed with 10% formaldehyde, and stored on ice until enumeration (maximum 3 hours).
173 Temperature, salinity, pH, and dissolved oxygen were measured using a handheld YSI 556
174 multiprobe system (YSI Inc., Ohio, USA). All metadata is available in Table S1.

175

176 *Dilution-to-extinction culturing and propagation*

177 Isolation, propagation, and identification of isolates were completed as previously reported (29,
178 35). A subsample of 2.7 μm filtered surface water was stained with 1X SYBR Green (Lonza,
179 Basal, Switzerland), and enumerated using a flow cytometer as described (60). After serial
180 dilution to a predicted 1-3 cells $\cdot \mu\text{l}^{-1}$, 2 μl water was inoculated into five, 96-well PTFE plates
181 (Radleys, Essex, UK) containing 1.7 ml artificial seawater medium (Table S1) to achieve an
182 estimated 1-3 cells $\cdot \text{well}^{-1}$ (Table 1). The salinity of the medium was chosen to match *in situ*
183 salinity after experiment JLB (January 2015) (Table S1). After year two (TBON3-LKB3), a
184 second generation of media, designated MWH, was designed to incorporate additional important

185 osmolytes, reduced sulfur compounds, and other constituents (Table S1) potentially necessary
186 for *in vitro* growth of uncultivated clades (49, 61–67). Cultures were incubated at *in situ*
187 temperatures (Table S1) in the dark for three to six weeks and evaluated for positive growth ($>$
188 10^4 cells·ml⁻¹) by flow cytometry. 200 µl from positive wells was transferred to duplicate 125 ml
189 polycarbonate flasks (Corning, New York, USA) containing 50 ml of medium. At FWC, FWC2,
190 JLB2c, and JLB3, not all positive wells were transferred because of the large number of positive
191 wells. At each site, 48/301, 60/403, 60/103, and 60/146 of the positive wells were transferred,
192 respectively, selecting for flow cytometric signals that maximized our chances of isolating small
193 microorganisms that encompass many of the most abundant, and most wanted taxa, like SAR11.
194

195 *Culture identification*

196 Cultures reaching $\geq 1 \times 10^5$ cells·ml⁻¹ had 35 ml of the 50 ml volume filtered for identification
197 via 16S rRNA gene PCR onto 25 mm 0.22-µm polycarbonate filters (Millipore, Massachusetts,
198 USA). DNA extractions were performed using the MoBio PowerWater DNA kit (QIAGEN,
199 Massachusetts, USA) following the manufacturer's instructions and eluted in sterile water. The
200 16S rRNA gene was amplified as previously reported in Henson et al. 2016 (35) and sequenced
201 at Michigan State University Research Technology Support Facility Genomics Core. Evaluation
202 of Sanger sequence quality was performed with 4Peaks (v. 1.7.1)
203 (<http://nucleobytes.com/4peaks/>) and forward and reverse complement sequences (converted via
204 http://www.bioinformatics.org/sms/rev_comp.html) were assembled where overlap was
205 sufficient using the CAP3 web server (<http://doua.prabi.fr/software/cap3>).
206

207 *Community iTag sequencing, operational taxonomic units, and single nucleotide variants*

208 Sequentially (2.7µm, 0.22µm) filtered duplicate samples were extracted and analyzed using our
209 previously reported protocols and settings (35, 68). We sequenced the 2.7-0.22 µm fraction for
210 this study because this fraction corresponded with the < 2.7 µm communities that were used for
211 the DTE experiments. To avoid batch sequencing effects, DNA from the first seven collections
212 reported in (35) was resequenced with the additional samples from this study (FWC2 and after-
213 Table 1). We targeted the 16S rRNA gene V4 region with the 515F, 806RB primer set (that
214 corrects for poor amplification of taxa like SAR11) (69, 70) using Illumina MiSeq 2 x 250bp
215 paired-end sequencing at Argonne National Laboratories, resulting in 2,343,106 raw reads for
216 the 2.7-0.22 µm fraction. Using Mothur v1.33.3 (71), we clustered 16S rRNA gene amplicons
217 into distinctive OTUs with a 0.03 dissimilarity threshold (OTU_{0.03}) and classified them according
218 to the Silva v119 database (72, 73). After these steps, 55,256 distinct OTU_{0.03} remained. We
219 also used minimum entropy decomposition (MED) to partition reads into fine-scale amplicon
220 single nucleotide variants (ASVs) (74). Reads were first analyzed using Mothur as described
221 above up to the *screen.seqs()* command. The cleaned reads fasta file was converted to MED-
222 compatible headers with the 'mothur2oligo' tool *renamer.pl* from the functions in MicrobeMiseq
223 (<https://github.com/DenefLab/MicrobeMiseq>) (75) using the fasta output from *screen.seqs()* and
224 the Mothur group file. These curated reads were analyzed using MED (v. 2.1) with the flags -M
225 60, and -d 1. MED resulted in 2,813 refined ASVs. ASVs were classified in Mothur using
226 *classify.seqs()*, the Silva v119 database, and a cutoff bootstrap value of 80% (76). After
227 classification, we removed ASVs identified as "chloroplast", "mitochondria", or "unknown"
228 from the dataset.
229

230 *Community analyses*

231 OTU (OTU_{0.03}) and ASV abundances were analyzed within the R statistical environment v.3.2.1
232 (77) following previously published protocols (29, 35, 68). Using the package PhyloSeq (78),
233 OTUs and ASVs were rarefied using the command *rarefy_even_depth()* and OTUs/ASVs
234 without at least two reads in four of the 34 samples (2 sites; ~11%) were removed. This cutoff
235 was used to remove any rarely occurring or spurious OTUs/ASVs. Our modified PhyloSeq
236 scripts are available on our GitHub repository <https://github.com/thrash-lab/Modified-Phyloseq>.
237 After filtering, the datasets contained 777 unique OTUs and 1,323 unique ASVs (Table S1). For
238 site-specific community comparisons, beta diversity between sites was examined using Bray-
239 Curtis distances via ordination with non-metric multidimensional scaling (NMDS) (Table S1).
240 The nutrient data were normalized using the R function *scale* which subtracts the mean and
241 divides by the standard deviation for each column. The influence of the transformed
242 environmental parameters on beta diversity was calculated in R with the *envfit* function. Relative
243 abundances of an OTU or ASV from each sample were calculated as the number of reads over
244 the sum of all the reads in that sample. The relative abundance was then averaged between
245 biological duplicates for a given OTU or ASV. To determine the best matching OTU or ASV for
246 a given LSUCC isolate, the OTU representative fasta file, provided by Mothur using
247 *get.oturep()*, and the ASV fasta file were used to create a BLAST database (*makeblastdb*) against
248 which the LSUCC isolate 16S rRNA genes could be searched via *blastn* (BLAST v 2.2.26)
249 (“OTU_ASVrep_db” - Available as Supplemental Information at
250 <https://doi.org/10.6084/m9.figshare.12142098>). We designated a LSUCC isolate 16S rRNA gene
251 match with an OTU or ASV sequence based on $\geq 97\%$ or $\geq 99\%$ sequence identity, respectively,
252 as well as a ≥ 247 bp alignment.

253 254 *16S rRNA gene phylogeny*

255 Taxa in the *Alpha*-, *Beta*-, and *Gammaproteobacteria* phylogenies from (35) served as the
256 backbone for the trees in the current work. For places in these trees with poor representation near
257 isolate sequences, additional taxa were selected by searching the 16S rRNA genes of LSUCC
258 isolates against the NCBI nt database online with BLASTn (79) and selecting a variable number
259 of best hits. The *Bacteroidetes* and *Actinobacteria* trees were composed entirely of non-
260 redundant top 100-300 MegaBLAST hits to a local version of the NCBI nt database, accessed
261 August 2018. Sequences were aligned with MUSCLE v3.6 (80) using default settings, culled
262 with TrimAl v1.4.rev22 (81) using the *-automated1* flag, and the final alignment was inferred
263 with IQ-TREE v1.6.11 (82) with default settings and *-bb 1000* for ultrafast bootstrapping (83).
264 Tips were edited with the *nw_rename* script within Newick Utilities v1.6 (84) and trees were
265 visualized with Archaeopteryx (85). Fasta files for these trees and the naming keys are available
266 as Supplemental Information at <https://doi.org/10.6084/m9.figshare.12142098>.

267 268 *Assessment of isolate novelty*

269 We quantified taxonomic novelty using BLASTn of our isolate 16S rRNA genes to those of
270 other known isolates collected in three databases: 1) The NCBI nt database (accessed August
271 2018) - “NCBIdb”; 2) a custom database comprised of sequences from other DTE experiments -
272 “DTEdb”; and 3) a database containing all our isolate 16S rRNA genes - “LSUCCdb”. The
273 DTEdb and LSUCCdb fasta files are available as Supplemental Information at
274 <https://doi.org/10.6084/m9.figshare.12142098>. We compared our isolate sequences to these
275 databases as follows:

- 276 1) All representative sequences were searched against the nt database using BLASTn
277 (BLAST+v. 2.7.1) with the flags -perc_identity 84, -evalue 1E-6, -task blastn, -outfmt “6
278 qseqid sseqid pident length slen qlen mismatch evalue bitscore sscinames sbblastnames
279 stitle”, and -negative_gilist to remove uncultured and environmental sequences. The
280 negative GI list was obtained by searching “environmental samples”[organism] OR
281 metagenomes[orgn]” in the NCBI Nucleotide database (accessed September 12th, 2018)
282 and hits were downloaded in GI list format. This negative GI list is available as
283 Supplemental Information at <https://doi.org/10.6084/m9.figshare.12142098>. The resultant
284 hits from the nt database search were further manually curated to remove sequences
285 classified as single cell genomes, clones, duplicates, and previously deposited LSUCC
286 isolates.
- 287 2) We observed that many known HTCC, IMCC, and HIMB isolates that had previously
288 been described as matching our clades (Figs. S1-5) were missing from the resultant lists
289 of nt hits, so we extracted isolate accession numbers from numerous DTE experiments
290 (26–28, 31, 34, 37, 44, 86, 87) from the nt database via *blastdbcmd* and generated a
291 separate DTEdb using *makeblastdb*. Duplicate accession numbers found in the NCBIdb
292 were removed. The same BLASTn settings as in 1) were used to search our isolate
293 sequences against DTEdb. Any match that fell below the lowest percent identity hit to the
294 NCBIdb was removed from the DTEdb search since the match would not have been
295 present in the first NCBIdb search.
- 296 3) Finally, using the same BLASTn settings, we compared all pairwise identities of our 328
297 LSUCC isolate 16S rRNA gene sequences via the LSUCCdb.

298 The output from these searches is available in Table S1 under the “taxonomic novelty” tab.

299 We placed our LSUCC isolates into 55 taxonomic groups based on sharing $\geq 94\%$
300 identity and/or their occurrence in monophyletic groups within our 16S rRNA gene trees (Figs.
301 S1-5, see above). For visualization purposes, in groups with multiple isolates we used our
302 chronologically first cultivated isolate as the representative sequence for blastn searches, and
303 these are the top point (100% identity to itself) in each group column of Figure 1. Sequences
304 from the other DTE culture collections were labeled with the corresponding collection name,
305 while all other hits were labeled as “Other”.

306 Geographic novelty was assessed by manually screening the accession numbers from hits
307 to LSUCC isolates with $\geq 99\%$ 16S rRNA gene sequence identity for the latitude and longitude
308 from a connected publication or location name (e.g. source, country, site) in the NCBI
309 description. LSUCC isolates in the *Janibacter* sp., *Micrococcus* sp., *Altererythrobacter* sp.,
310 *Pseudomonas* sp., and *Phycoccus* sp. groups (16 total isolates) were not assessed because of
311 missing isolation source information and no traceable publication.

312 313 *Modeling DTE cultivation via Monte Carlo simulations*

314 We developed a model using Monte Carlo simulation to estimate the median number of positive
315 and pure wells (and associated 95% confidence intervals (CI)) expected from a DTE experiment
316 for a given taxon at different inoculum sizes (λ), relative abundances (r), and viability (V) (Fig.
317 5). For each bootstrap, the number of cells added to each well was simulated using a Poisson
318 distribution at a mean inoculum size of λ cells per well across n wells. The number of cells added
319 to each well that belonged to a specific taxon was then estimated using a binomial distribution
320 where the number of trials was set as the number of cells in a well and the probability of a cell
321 belonging to a specific taxon, r , was the relative abundance of its representative ASV in the

322 community analysis. Wells that contained at least one cell of a specific taxon were designated
323 ‘positive’. Wells in which all the cells belonged to a specific taxon were designated as ‘pure’.
324 Finally, the influence of taxon-specific viability on recovery of ‘pure’ wells was simulated using
325 a second binomial distribution, where the number of cells within a ‘pure’ well was used as the
326 number of trials and the probability of growth was a viability score ranging from 0 to 1. For each
327 simulation, 9,999 bootstraps were performed. Code for the model and all simulations is available
328 in the ‘viability_test.py’ at our GitHub repository https://github.com/thrash-lab/viability_test.

329

330 *Actual versus expected number of isolates*

331 For each taxon in each DTE experiment, the Monte Carlo simulation was used to evaluate
332 whether the number of recovered pure wells for each taxon was within 95% CI of simulated
333 estimates, assuming optimum growth conditions (i.e. $V = 100\%$). For each of 9,999 bootstraps,
334 460 wells were simulated with the inoculum size used for the experiment and the relative
335 abundance of the ASV. For taxa where the number of expected wells fell outside the 95% CI of
336 the model, a deviance score was calculated as the difference between the actual number of wells
337 observed and median of the simulated dataset. The results of this output are presented in Table
338 S1 under the “Expected vs actual” tab, and the R script for visualizing this output as Figure 6 is
339 available at our GitHub repository <https://github.com/thrash-lab/EvsA-visualization>.

340

341 *Estimating viability in under-represented taxa*

342 For taxa where the observed number of positive wells was lower than the 95% CI lower limit
343 within a given experiment, and because our analysis was restricted to only those organisms for
344 which our media was sufficient for growth at least once, the deviance was assumed to be a
345 function of a viability term, V , (ranging from 0 to 1) associated with suboptimal growth
346 conditions, dormancy, persister cells, etc. To estimate a value of viability for a given taxon
347 within a particular experiment, the Monte Carlo simulation was run using an experiment-
348 appropriate inoculum size, relative abundance, and number of wells (460 for each experiment).
349 Taxon-specific viability was tested across a range of decreasing values from 99% to 1% until
350 such time as the observed number of pure wells for a given taxon fell between the 95% CI
351 bounds of the simulated data. At this point, the viability value is the maximum viability of the
352 taxon that enables the observed number of pure wells for a given taxon to be explained by the
353 model. The results of this output are presented in Table S1 under the “Expected vs actual” tab.

354

355 *Likelihood of recovering taxa at different relative abundances*

356 To estimate the number of wells required in a DTE experiment to have a significant chance of
357 recovering a taxon with a relative abundance of r , assuming optimum growth conditions ($V =$
358 100%), the Monte Carlo model was used to simulate experiments from 92 wells to 9,200 wells
359 per experiment across a range of relative abundances from 0 to 100% in 0.1% increments, and a
360 range of inoculum sizes (cells per well of 1, 1.27, 1.96, 2, 3, 4 and 5). Each experiment was
361 bootstrapped 999 times and the number of bootstraps in which the lower-bound of the 95% CI
362 was ≥ 1 was recorded.

363

364 *Data accessibility*

365 All iTag sequences are available at the Short Read Archive with accession numbers
366 SRR6235382-SRR6235415 (29). PCR-generated 16S rRNA gene sequences from this study are
367 accessible on NCBI GenBank under the accession numbers MK603525-MK603769. Previously

368 generated 16S rRNA genes sequences are accessible on NCBI GenBank under the accession
 369 numbers KU382357-KU38243 (35). Table S1 is available at
 370 <https://doi.org/10.6084/m9.figshare.12142113>.

371
 372 **Results**

373 *General cultivation campaign results*

374 We conducted a total of seventeen DTE cultivation experiments to isolate bacterioplankton (sub
 375 2.7 μm fraction), with paired microbial community characterization of source waters (0.22 μm -
 376 2.7 μm fraction), from six coastal Louisiana sites over a three year period (Table S1). We
 377 inoculated 7,820 distinct cultivation wells (all experiments) with an estimated 1-3 cells \cdot well $^{-1}$
 378 using overlapping suites of artificial seawater media, JW (years 1 and 2, (35)) and MWH (year
 379 3), designed to match the natural environment (Table 1). The MWH suite of media was modified
 380 from the JW media to additionally include choline, glycerol, glycine betaine, cyanate, DMSO,
 381 DMSP, thiosulfate, and orthophosphate. These compounds have been identified as important
 382 metabolites and osmolytes for marine and freshwater prokaryotes and were absent in the first
 383 iteration (JW) of our media (Table S1) (88–94). A total of 1,463 wells were positive ($> 10^4$
 384 cells \cdot ml $^{-1}$), and 738 of these were transferred to 125 mL polycarbonate flasks. For four
 385 experiments (FWC, FWC2, JLB2, and JLB3) we only transferred a subset of positives (48/301,
 386 60/403, 60/103, and 60/146) because the number of isolates exceeded our ability to maintain and
 387 identify them at that time (Table 1). The subset of positive wells for these four experiments was
 388 selected using flow cytometry signatures with $< 10^2$ green fluorescence and $< 10^2$ side scatter-
 389 usually indicative of smaller oligotrophic cells like SAR11 strain HTCC1062 (49) using our
 390 settings. Of the 738 wells from which we transferred cells across all experiments, 328 of these
 391 yielded repeatably transferable isolates that we deemed as pure cultures based on 16S rRNA
 392 gene PCR and Sanger sequencing.

393
 394

Table 1. Cultivation statistics, including whole community viability estimates

Site	Date	n	z	p	λ	V^* (ASE)	CV	our model: estimated # wells with 1 cell (bootstrapped median: (xx-xx) 95% CI) if $V^*=1$ **	our model: V_{est} : min- max 95% CI ***	<i>in situ</i> salinity	Medium salinity	Medium JWAMPF e	Study
CJ	Sep 2014	460	15	0.033	1.27	2.6 (0.67)	0.259	164 (144-185)	1.5-4.2	24.6	34.8	JWAMPF e	(35)
ARD	Nov 2014	460	1	0.002	1.5	0.1 (0.15)	1.451	154 (134-174)	0.1-0.7	1.72	34.8	JW1	(35)
JLB	Jan 2015	460	61	0.133	1.96	7.3 (0.93)	0.127	127 (109-146)	5.6-9.2	26.0	34.8	JW1	(35)
FWC †	Mar 2015	460	301	0.654	2	53.1 (3.2)	0.06	125 (106-143)	47.1-59.7	5.39	5.79	JW4	(35)
LKB	June 2015	460	15	0.033	1.8	1.8 (0.48)	0.266	137 (118-156)	1.1-3.0	2.87	5.79	JW4	(35)
Tbon2	Aug 2015	460	41	0.089	1.56	6.0 (0.93)	0.156	151 (132-171)	4.3-8.1	14.2	11.6	JW3	(35)
CJ2	Oct 2015	460	61	0.133	2	7.1 (0.91)	0.128	125 (106-143)	5.6-9.1	22.2	23.2	JW2	(35)
FWC2 †	Apr 2016	460	403	0.876	2	104.4 (6.2)	0.059	125 (106-143)	>92.3	20.9	23.2	JW2	This study
ARD2c	Jun 2016	460	7	0.015	2	0.8 (0.29)	0.362	125 (106-143)	0.3-1.5	0.18	1.45	JW5	This study
JLB2c †	May 2016	460	103	0.224	2	12.7 (1.25)	0.099	125 (106-143)	10.3-15.4	6.89	5.79	JW4	This study
LKB2	Jul 2016	460	39	0.085	2	4.4 (0.71)	0.161	125 (106-143)	3.2-6.0	2.39	1.45	JW5	This study
Tbon3	Jul 2016	460	78	0.17	2	9.3 (1.05)	0.113	125 (106-143)	7.4-11.5	17.7	34.8	MWH1	This study
CJ3	Sep 2016	460	69	0.15	2	8.1 (0.98)	0.121	125 (106-143)	6.4-10.2	23.7	23.2	MWH2	This study
FWC3	Nov 2016	460	27	0.059	2	3.0 (0.58)	0.194	125 (106-143)	2.0-4.4	18.0	23.2	MWH2	This study
ARD3	Dec 2016	460	58	0.126	2	6.7 (0.89)	0.132	125 (106-143)	5.2-8.6	3.72	1.45	MWH5	This study
JLB3 †	Jan 2017	460	146	0.317	2	19.1 (1.59)	0.083	125 (106-143)	16.1-22.4	12.4	11.6	MWH3	This study
LKB3	Feb 2017	460	38	0.083	2	4.3 (0.70)	0.163	125 (106-143)	3.1-5.8	3.55	1.45	MWH5	This study

395 *Viability according to equation 1, above. Asymptotic Standard Error (ASE) is presented in parentheses.

396 **Based on 9,999 bootstraps.
397 ***Based on 9,999 bootstraps tested at viability increments of 0.1%.
398 †Experiments where a subset of positive wells were transferred.
399 FWC2 shows the advantage of our method over equation 1 for extreme values.

400

401 *Phylogenetic and geographic novelty of our isolates*

402 The 328 isolates belonged to three Phyla: *Proteobacteria* (n = 319), *Actinobacteria* (n = 8), and
403 *Bacteroidetes* (n = 1) (Figs. S1-S5). We placed these isolates into 55 groups based on their
404 positions within 16S rRNA gene phylogenetic trees (Figs. S1-S5) and as a result of having \geq
405 94% 16S rRNA gene sequence identity to other isolates. We applied a nomenclature to each
406 group based on previous 16S rRNA gene database designations and/or other cultured
407 representatives (Fig. 1, Table S1). Isolates represented eight putatively novel genera with \leq
408 94.5% 16S rRNA gene identity to a previously cultured representative: the *Actinobacteria* acIV
409 subclades A and B, and one other unnamed *Actinobacteria* group; an undescribed
410 *Acetobacteraceae* clade (*Alphaproteobacteria*); the freshwater SAR11 LD12 (*Candidatus*
411 *Fonsibacter ubiquis* (29)); the MWH-UniPo and an unnamed *Burkholderiaceae* clade
412 (*Betaproteobacteria*); and the OM241 *Gammaproteobacteria* (Fig. 1, Table S1). Seven
413 additional putatively novel species were also cultured (between 94.6 and 96.9% 16S rRNA gene
414 sequence identity) in unnamed *Commamonadaceae* and *Burkholderiales* clades
415 (*Betaproteobacteria*); the SAR92 clade and *Pseudohonigella* genus (*Gammaproteobacteria*); and
416 unnamed *Rhodobacteraceae* and *Bradyrhizobiaceae* clades, as well as *Maricaulis* spp.
417 (*Alphaproteobacteria*) (Fig. 1). LSUCC isolates belonging to the groups BAL58
418 *Betaproteobacteria* (Fig. S4), OM252 *Gammaproteobacteria*, HIMB59 *Alphaproteobacteria*,
419 and what we designated the LSUCC0101-type *Gammaproteobacteria* (Fig. S5) had close 16S
420 rRNA gene matches to other cultivated taxa at the species level, however, none of those
421 previously cultivated organisms have been formally described (Fig. 1). The OM252, BAL58, and
422 MWH-UniPo clades were the most frequently cultivated, with 124 of our 328 isolates belonging
423 to these three groups (Table S1). In total, 73 and 10 of the 328 isolates belonged in putatively
424 novel genera and species, respectively. We estimated that at least 310 of these isolates were
425 geographically novel, being the first of their type cultivated from the nGOM (Fig. 2). This
426 included isolates from cosmopolitan groups like SAR11 subclade IIIa, OM43
427 *Betaproteobacteria*, SAR116, and HIMB11-type “Roseobacter” spp.. Cultivars from *Vibrio* sp.
428 and *Alteromonas* sp. were the only two groups that contained hits to organisms isolated from the
429 GoM.

430

431 *Natural abundance of isolates*

432 We matched LSUCC isolate 16S rRNA gene sequences with both operational taxonomic units
433 (OTUs) and amplicon single nucleotide variants (ASVs) from bacterioplankton communities to
434 assess the relative abundances of our isolates in the coastal nGOM waters that served as inocula.
435 While OTUs provide a broad group-level designation (97% sequence identity), this approach can
436 artificially combine multiple ecologically distinct taxa (95). Due to higher stringency for
437 defining a matching 16S rRNA gene, ASVs can increase the confidence that our isolates
438 represent environmentally relevant organisms (74, 96). However, while many abundant
439 oligotrophic bacterioplankton clades such as SAR11 (29, 97), OM43 (40, 41), SAR116 (98), and
440 *Sphingomonas* spp. (99) have a single copy of the rRNA gene operon, other taxa can have
441 multiple rRNA gene copies (97, 100), complicating ASV analyses. Since we could not *a priori*

442 rule out multiple rRNA gene operons for novel groups with no genome sequenced
443 representatives, we used both OTU and ASV approaches.

444 In total, we obtained at least one isolate from 40 of the 777 OTUs and 71 of the 1,323
445 ASVs observed throughout the three-year dataset. 43% and 26% of LSUCC isolates matched the
446 top 50 most abundant OTUs (median relative abundances, all sites, from 0.11-8.1%; Fig. S6A)
447 and ASVs (mean relative abundances, all sites, from 0.11-3.8%; Fig. S6B), respectively, across
448 all sites and samples. Microbial communities from all collected samples clustered into two
449 groups corresponding to those inhabiting salinities below 7 and above 12, and salinity was the
450 primary environmental driver distinguishing community beta diversity (OTU: $R^2=0.88$, $P=0.001$,
451 ASV: $R^2=0.89$, $P=0.001$). As part of the cultivation strategy after the first five experiments, we
452 used a suite of five media differing by salinity and matched the experiment with the medium that
453 most closely resembled the salinity at the sample site. Consequently, our isolates matched
454 abundant environmental groups from both high and low salinity regimes. At salinities above
455 twelve, LSUCC isolates matched 13 and 14 of the 50 most abundant OTUs and ASVs,
456 respectively (Figs. 3A, 3B; Table S1). These taxa included the abundant SAR11 subclade IIIa.1,
457 HIMB59, HIMB11-type “Roseobacter”, and SAR116 *Alphaproteobacteria*; the OM43
458 *Betaproteobacteria*; and the OM182 and LSUCC0101-type *Gammaproteobacteria*. At salinities
459 below seven, 10 and 9 of the 50 most abundant OTUs and ASVs, respectively, were represented
460 by LSUCC isolates, including one of most abundant taxa in both cluster sets, SAR11 LD12
461 (Figs. 3C, 3D). Some taxa, such as SAR11 IIIa.1 and OM43, were among the top 15 most
462 abundant taxa in both salinity regimes (Fig. 3, Table S1), suggesting a euryhaline lifestyle. In
463 fact, our cultured SAR11 IIIa.1 ASV7471 was the most abundant ASV in the aggregate dataset
464 (Fig. S6).

465 Overall, this effort isolated taxa representing 18 and 12 of the top 50 most abundant
466 OTUs and ASVs, respectively (Table 2, Fig. S6). When looking at different median relative
467 abundance categories of $> 1\%$, $0.1\% - 1\%$, and $< 0.1\%$, isolate OTUs were distributed across
468 those categories in the following percentages: 15%, 20%, and 27%; isolate ASVs were
469 distributed accordingly: 4%, 26%, and 37% (Table 2). Isolates with median relative abundances
470 of $< 0.1\%$, such as *Pseudohongiella* spp., *Rhodobacter* spp., and *Bordetella* spp., would
471 canonically fall within the rare biosphere (101) (Table S1). A number of isolates did not match
472 any identified OTUs or ASVs (38% and 33% of LSUCC isolates when compared to available
473 OTUs and ASVs, respectively), either because their matching OTUs/ASVs were below our
474 thresholds for inclusion (at least two reads from at least two sites), or because they were below
475 the detection limit from our sequencing effort (Table 2). Thus, 43% and 30% of our isolates
476 belonged to OTUs and ASVs, respectively, with median relative abundances $> 0.1\%$.

477

478 **Table 2. Median relative abundances (r) of cultured OTUs and ASVs across all samples**

	In top 50 ranks	$r > 1\%$	$1\% - 0.1\% r$	$r < 0.1\%$	Not detected
OTUs	18 (140 isolates)	50 isolates (15%)	90 isolates (27%)	65 isolates (20%)	123 isolates (38%)
ASVs	12 (84 isolates)	13 isolates (4%)	84 isolates (26%)	122 isolates (37%)	109 isolates (33%)

479

480 *Modeling DTE cultivation*

481 An enigma that became immediately apparent through a review of our data was the absence of an
482 obvious relationship between the abundance of a given taxon in the inoculum and the frequency
483 of obtaining an isolate of the same type from a DTE cultivation experiment (Figs. S7, S8). For
484 example, although we could culture SAR11 LD12 over a range of media conditions (29), and the
485 matching ASV had relative abundances of $> 5\%$ in six of our seventeen experiments (Fig. 4), we

486 only isolated one representative (LSUCC0530). In an ideal DTE cultivation experiment where
487 cells are randomly subsampled from a Poisson-distributed population, if the medium were
488 sufficient for a given microorganism's growth, then the number of isolates should correlate with
489 that microorganism's abundance in the inoculum. However, a qualitative examination of several
490 abundant taxa that grew in our media, some of which we cultured on multiple occasions,
491 revealed no clear pattern between abundance and isolation success (Fig. 4). Considering that
492 medium composition was sufficient for cultivation of these organisms on at least some
493 occasions, we hypothesized that cultivation frequency may reflect viability differences in the
494 populations of a given taxon. Thus, we decided to model cultivation frequency in relationship to
495 estimated abundances in a way that could generate estimates of cellular viability. We also hoped
496 that this information might help us inform experimental design and make DTE cultivation efforts
497 more predictable (59).

498 Previously, Don Button and colleagues developed a statistical model for viability (V) of
499 cells in the entire sample for a DTE experiment (33):

500

$$501 \quad (1) \quad V = -(\ln(1-p)/\lambda)$$

502

503 Where p is the proportion of wells or tubes, n , with growth, z , ($p=z/n$) and λ is the estimated
504 number of cells inoculated per well (the authors used X originally). The equation uses a Poisson
505 distribution to account for the variability in cell distribution within the inoculum and therefore
506 the variability in the number of wells or tubes receiving the expected number of cells. We and
507 others have used this equation in the past (26, 28, 35) to evaluate the efficacy of our cultivation
508 experiments in the context of commonly cited numbers for cultivability using agar-plate based
509 methods (13, 17, 102).

510 While Equation 1 is effective for its intended purpose, it has a number of drawbacks that
511 limit its utility for taxon-specific application: 1) If $p=1$, i.e. all wells are positive, then the
512 equation is invalid; 2) At high values of p and low values of λ , estimates of V can exceed 100%
513 (Table 2); 3) Accuracy of viability, calculated by the asymptotic standard error, $ASEV$, or the
514 coefficient of variation, CVV , was shown to be non-uniform across a range of λ , with greatest
515 accuracy when true viability was ~10% (33). Thus, low viability, low values of λ , and small
516 values of n were found to produce unreliable results; 4) If $p=0$, i.e. no positive wells are
517 observed, estimates of viability that could produce 0 positive wells cannot be calculated. In
518 addition, 5) Button's original model assumes that a well will only produce a pure culture if the
519 inoculated well contains one cell. By contrast, in low diversity samples, samples dominated by a
520 single taxon, or experiments evaluating viability from axenic cultures across different media, a
521 limitation that only wells with single cells are axenic will underestimate the expected number of
522 pure wells. To overcome these limitations, we developed a Monte Carlo simulation model that
523 facilitates the incorporation of relative abundance data from complementary community profiling
524 data (e.g. 16S rRNA gene amplicons) to calculate the likelihood of positive wells, pure wells,
525 and viability at a taxon-specific level, based on the observed number of wells for we obtained an
526 isolate of a particular taxon (Fig. 5). By employing a Monte Carlo approach, our model is robust
527 across all values of p and n with uniform prediction accuracy, and we can estimate the accuracy
528 of our prediction within 95% confidence intervals (CI). Furthermore, the width of 95% CI
529 boundaries of viability, as well as the expected number of positive and pure wells, are entirely
530 controllable and dependent only on available computational capacity for bootstrapping (i.e.,
531 these can be improved with more bootstrapping, but at greater computational cost). When zero

532 positive wells are observed experimentally, our approach enables estimation of a maximum
533 viability that could explain such an observation by identifying the range of variability values for
534 which zero resides within the bootstrapped 95% CI. Finally, the ability to calculate the viability
535 of the entire community, as in Equation 1, is retained simply by estimating viability using a
536 relative abundance of one.

537 We compared our model to that of Button et al. for evaluating viability from whole
538 community experimental results, similarly to previous reports (26, 28, 35) (Table 1). Our
539 viability estimates (V_{est}) generally agreed with those using the Button et al. calculation, but we
540 have now provided 95% CI to depict the maximum and minimum viability that would match the
541 returned positive well distribution, as well as maximum and minimum values for the number of
542 wells that ought to have contained a single cell. Maximum V_{est} ranged from 1.1% to > 92.3%
543 depending on the experiment, with a median V_{est} across all our experiments of 8.6% (Table 1). In
544 one case, the extremely high value (FWC2) was better handled by our model compared to
545 equation 1, because it did not lead to a viability estimation greater than 100%. FWC and FWC2
546 represent V_{est} outliers compared with the entire dataset (maximums of 59.7% and > 92.3%,
547 respectively; Table 1). We believe these high numbers most likely resulted from underestimating
548 the number of cells inoculated into each well because of the use of microscopy, clumped cells, or
549 pipet error, thus increasing the estimated viability (35).

550

551 *Isolate-specific viability estimates*

552 Our new model also facilitates taxon-specific viability estimates. Cultivation efficacy was
553 evaluated for 71 cultured ASVs (219 isolates) across 17 sites (1,207 pairwise combinations) by
554 comparing the number of observed pure wells to those predicted by the Monte Carlo simulation
555 using 9,999 bootstraps, 460 wells per experiment, and an assumption that all cells were viable
556 (i.e. $V = 100\%$). In total, for 1,158 out of 1,207 pairwise combinations (95.9%) the observed
557 number of pure wells fell within the 95% CI of data simulated at matching relative abundance
558 and inoculum size, suggesting that these two parameters alone could explain the observed
559 cultivation success for most taxa (Table S1). 1,059 out of these 1,158 combinations (91%)
560 recorded zero observed wells, but with a maximum relative abundance of 2.8% within these
561 combinations, a score of zero fell within predicted 95% CI of simulations with 460 wells.
562 Sensitivity analysis showed that with 460 wells per experiment, an observation of zero pure
563 wells falls below the 95% confidence intervals lower-bound (and is thus significantly depleted to
564 enable viability to be estimated) for taxa with relative abundances of 2.3%, 2.9% and 4.5% for
565 inoculum sizes of one, two and three cells per well, respectively (Fig. S9). In fact, modeling DTE
566 experiments from 92 wells to 9,200 wells per experiment showed that for taxa comprising ~1%
567 of a microbial community 1,104 wells (or 12 plates at 92 wells per plate), 1,380 wells (15 plates)
568 and 2,576 wells (28 plates) were required to be statistically likely to recover at least one positive,
569 pure well using inocula of one, two or three cells per well, respectively, with $V = 100\%$ (Fig. S9).

570 A small, but taxonomically relevant minority (49 out of 1,207) of pairwise combinations
571 had a number of observed pure wells that fell outside of the simulated 95% CI with $V = 100\%$
572 (Fig. 6). Of these, 28 had either one, two, or three more observed pure wells than the upper 95%
573 CI (Table S1), suggesting cultivability *higher* than expected based purely a model capturing the
574 interaction between a Poisson-distributed inoculum and a binomially-distributed relative
575 abundance, with $V = 100\%$. However, the deviance from the expected number of positive wells
576 for those above the 95% CI was limited to three or fewer cells, meaning that we only obtained 1-
577 3 more isolates than expected (Table S1). On the other hand, those organisms that we isolated

578 less frequently than expected showed greater deviance. 21 out of the 49 outliers had lower than
 579 expected cultivability (Fig. 6). These taxa had relative abundances ranging from 2.7% to 14.5%,
 580 but recorded only 0, 1, or 2 isolates. In the most extreme case, ASV7629 (SAR11 LD12) at Site
 581 ARD2c comprised 14.5% of the community but recorded no observed pure wells, compared to
 582 expected number of 13-30 isolates (95% CI) predicted by the Monte Carlo simulation. All the
 583 examples of taxa that were isolated less frequently than expected given the assumption of $V =$
 584 100% belonged to either SAR11 LD12, SAR11 IIIa.1, or one particular OM43 ASV (7241) (Fig.
 585 6).

586 We used our model to calculate estimated viability (V_{est}) for these organisms based on
 587 their cultivation frequency at sites where the assumption of $V = 100\%$ appeared violated (Table
 588 3). Using the extreme example of SAR11 LD12 ASV7629 at Site ARD2c, simulations across a
 589 range of V indicated that a result of zero positive wells fell within 95% of simulated values when
 590 the associated taxon $V_{est} \leq 15\%$. When considering all anomalous cultivation results, LD12 had
 591 estimated maximum viabilities that ranged up to 55% (Table 3). OM43 (ASV7241) estimated
 592 maximum viabilities ranged from 52-80%, depending on the site, and similarly, SAR11 IIIa.1
 593 ranged between 22-82% viability (Table 3).
 594
 595

Table 3. Estimated viabilities for taxa cultivated less frequently than expected

ASV	Group	Site	r^*	n	z	λ	Estimated # wells with 1 cell (bootstrapped median: (xx-xx) 95% CI) if $V=1$ **	V_{est} : min-max 95% CI based on cultivation results***
7241	OM43	ARD3	0.03	460	0	2	4 (1-9)	0.1-80
7241	OM43	FWC [†]	0.04	460	0	2	5 (1-9)	0.1-77
7241	OM43	JLB	0.05	460	0	1.96	7 (2-12)	0.1-52
7471	SAR11 IIIa.1	ARD3	0.11	460	0	2	15 (8-23)	0.1-22
7471	SAR11 IIIa.1	CJ	0.03	460	0	1.27	4 (1-9)	0.1-82
7471	SAR11 IIIa.1	FWC3	0.07	460	2	2	9 (4-15)	2.5-80
7471	SAR11 IIIa.1	JLB	0.05	460	0	1.96	6 (2-11)	0.1-59
7471	SAR11 IIIa.1	JLB2c [†]	0.08	460	0	2	11 (5-18)	0.1-31
7471	SAR11 IIIa.1	JLB3 [†]	0.04	460	0	2	5 (1-9)	0.1-74
7471	SAR11 IIIa.1	LKB	0.05	460	0	1.8	6 (2-12)	0.1-55
7471	SAR11 IIIa.1	LKB2	0.04	460	0	2	5 (1-9)	0.1-77
7471	SAR11 IIIa.1	LKB3	0.09	460	0	2	11 (6-19)	0.1-30
7471	SAR11 IIIa.1	TBON2	0.04	460	0	1.56	6 (2-12)	0.1-56
7471	SAR11 IIIa.1	TBON3	0.04	460	0	2	5 (1-10)	0.1-73
7629	SAR11 LD12	ARD	0.11	460	0	1.5	18 (10-27)	0.1-20
7629	SAR11 LD12	ARD2c	0.15	460	0	2	21 (13-30)	0.1-15
7629	SAR11 LD12	ARD3	0.05	460	0	2	7 (2-12)	0.1-53
7629	SAR11 LD12	FWC [†]	0.09	460	0	2	12 (6-19)	0.1-28
7629	SAR11 LD12	LKB	0.05	460	0	1.8	7 (2-13)	0.1-51
7629	SAR11 LD12	LKB2	0.08	460	1	2	11 (5-18)	0.3-49
7629	SAR11 LD12	LKB3	0.06	460	0	2	7 (3-13)	0.1-48

596 *Fractional relative abundance

597 **Based on 9,999 bootstraps.

598 ***Based on 9,999 bootstraps tested at viability increments of 0.1%.

599 [†]Experiments where a subset of positive wells were transferred.

600

601 Discussion

602 This work paired 17 DTE cultivation experiments with cultivation-independent assessments of
 603 microbial community structure in source waters to evaluate cultivation efficacy. We generated
 604 328 new bacterial isolates representing 40 of the 777 OTUs and 71 of the 1,323 ASVs observed
 605 across all samples from which we inoculated DTE experiments. Stated another way, we
 606 successfully cultivated 5% of the total three year bacterioplankton community observed via
 607 either OTU or ASV analyses. A large fraction of our isolates (43% of cultured OTUs, 30% of

608 cultured ASVs) represented taxa present at median relative abundances $> 0.1\%$, with 15% and
609 4% of cultured OTUs and ASVs, respectively, at median abundances $> 1\%$. 140 of our isolates
610 matched the top 50 most abundant OTUs, and 84 isolates matched the top 50 most abundant
611 ASVs.

612 This campaign led to the first isolations of the abundant SAR11 LD12 and *Actinobacteria*
613 acIV; the second isolate of the HIMB59 *Alphaproteobacteria*; and new genera within the
614 *Acetobacteraceae*, *Burkholderiaceae*, OM241 and LSUCC0101-type *Gammaproteobacteria*, and
615 MWH-UniPo *Betaproteobacteria*; thereby demonstrating again that continued DTE
616 experimentation leads to isolation of previously uncultured organisms with value for aquatic
617 microbiology. We have also added a considerable collection of isolates to previously cultured
618 groups like OM252 *Gammaproteobacteria*, BAL58 *Betaproteobacteria*, and HIMB11-type
619 “Roseobacter” spp., and the majority of our isolates represent the first versions of these types of
620 taxa from the Gulf of Mexico, adding comparative biogeographic value to these cultures.

621 Our viability model improved upon the statistical equation developed by Button and
622 colleagues (33) to extend viability estimates to individual taxa within a mixed community and
623 provide 95% CI constraining those viability estimates. We cultured several groups of organisms
624 abundant enough to evaluate viability with 460 wells (Figs. 6, S9). The fact that these organisms
625 were successfully cultured at least once meant that we could reasonably assume that the medium
626 was sufficient for growth. Some taxa were cultivated more frequently than expected (Fig. 6). We
627 explore two possible explanations for this phenomenon- errors in quantification and variation in
628 microbial cell organization. Any systematic error that led to underestimating the abundance of an
629 organism would have correspondingly resulted in our underestimating the number of wells in
630 which we would expect to find a pure culture of that organism. Such underestimations could
631 come from primer biases associated with amplicon sequencing (69, 70, 103), but we do not know
632 if those protocols specifically underestimate the OM252, MWH-UniPo, and HIMB11-type taxa
633 cultured more frequently than expected (Fig. 6). However, due the low number of expected
634 isolates in these groups, and the small deviances in actual isolates from those expected numbers
635 (within 1-3 isolates compared to expected values), the biases inherent in the relative abundance
636 estimations for these taxa were probably small. Furthermore, one of the microorganisms isolated
637 more frequently than expected matched the OM43 ASV1389 (Fig. S6), whereas another OM43
638 ASV (7241) was cultivated less frequently than expected (see below), meaning that if primer
639 bias were the cause of this discrepancy, it would have to be operating differently on very closely
640 related organisms.

641 There exists a biological explanation for why some isolates might have been cultured
642 more frequently than expected: clumped cells. If cells of any given taxon in nature grew in small
643 clusters, then the number of cells we added to a well was greater than expected based on a
644 Poisson distribution. Furthermore, the model assumes that each cell is independent, and that the
645 composition of a subset of cells is only a function of the relative abundance of the taxon in the
646 community. Within a cluster of cells, this assumption is violated as the probability of cells being
647 from the same taxon is higher. Thus, the model will underestimate the probability of a well being
648 pure and therefore underestimate the number of pure wells likely to be observed within an
649 experiment, leading to a greater number of isolates than expected. Future microscopy work could
650 examine whether microorganisms such as OM252 and MWH-UniPo form small clusters *in situ*
651 and/or in pure culture, and whether this phenomenon may be different for different ASVs of
652 OM43, or if clumping may be a transient phenotype.

653 We also identified three taxa- SAR11 LD12, SAR11 subclade IIIa.1, and the
654 aforementioned OM43 ASV7241- that were isolated much less frequently than expected based
655 on their abundances (Fig. 6, Table 3). This could mean that our assumption of $V = 100\%$ was
656 incorrect, or that, in contrast to the taxa that were cultured more frequently than expected
657 (above), our methods had biases that *overestimated* the abundance of these organisms, thereby
658 over-inflating the expected number of isolates. We used the modified 515/806RB primers that
659 have been shown to be much more accurate in quantifying SAR11 compared to FISH than the
660 original 515/806 primers (within $6\% \pm 4\%$ SD), and this protocol almost always underestimates
661 SAR11 abundances (69). This suggests that our expected number of isolates may have actually
662 been underestimated, our cultivation success was poorer than we measured, and therefore we
663 may be overestimating viability for the SAR11 taxa. Other sources of systematic error that might
664 impinge on successful transfers, and thereby reduce our recovery, include sensitivity to pipette
665 tip and/or flask material. However, the fact that these taxa were sometimes successfully isolated
666 means that if these mechanisms were impacting successful transfers, then their activity was less
667 than 100% efficient, which implies variations in subpopulation vulnerability that would be very
668 similar conceptually to variations in subpopulation viability.

669 Another possible source of error that could have resulted in lower than expected numbers
670 of isolates was the subset of experiments for which we did not transfer all positive wells due to
671 limitations in available personnel time (Tables 1 & 3). However, our selection criteria for the
672 subset of wells to transfer was based on flow cytometric signatures that would have encompassed
673 small cells like SAR11 (see Results), and in any case, there were many examples of lower than
674 expected recovery from other experiments where we transferred all positive wells (Table 3).
675 Therefore, these four experiments were unlikely to contribute major errors biasing our estimates
676 of viability for SAR11 LD12, SAR11 IIIa.1, and other small cells like OM43.

677 If we instead explore biological reasons for the lower than expected numbers of positive
678 wells in DTE experiments, a plausible explanation supported by the literature is simply that a
679 large fraction of the population is in some state of inactivity or at least not actively dividing
680 (104). Studies using uptake of a variety of radiolabelled carbon and sulfur sources have
681 demonstrated substantial fractions of SAR11 cells may be inactive depending on the population
682 (105–108). SAR11 cells in the northwest Atlantic and Mediterranean showed variable uptake of
683 labelled leucine (30-50% (105, 106); ~25-55% (108, 109) and amino acids (34-61% (105, 106);
684 34-66% (105, 106). Taken in reverse, this means that up to 75% of the SAR11 population may
685 be inactive at any given time. In another study focused on brackish communities, less than 10%
686 of SAR11 LD12 cells took up labelled leucine and/or thymidine (107). While this was likely not
687 the ideal habitat for LD12 based on salinities above 6 (29, 107), this study supports the others
688 above that show substantial proportions of inactive SAR11 cells, the fraction of which may
689 depend on environmental conditions and other unknown factors. Bi-orthogonal non-canonical
690 amino acid tagging (BONCAT) shows similar trends for SAR11 (110). These data also match
691 general data indicating prevalent inactivity among aquatic bacterioplankton (104, 111–113).
692 Although labelled uptake methods do not directly measure rates of cell division, the
693 incorporation of these compounds requires active DNA replication or translation, which
694 represent an even more fundamental level of activity than cell division (114).

695 Why might selection favor low viability? One possibility is as an effective defense
696 mechanism against abundant viruses. Viruses infecting SAR11 have been shown to be extremely
697 abundant in both marine (115, 116) and freshwater (117) systems. Indeed, the paradox of high
698 viral abundances and high host abundances in SAR11 has led to a refining of negative density

699 dependent selection through Lotka-Volterra predator-prey dynamics (118) to include
700 heterogeneous susceptibility at the strain level (119, 120) and positive density dependent
701 selection through intraspecific proliferation of defense mechanisms (121). Activity of lytic
702 viruses infecting SAR11 *in situ* demonstrated that phages infecting SAR11 have lower ratios of
703 viral transcripts to host cells compared to other abundant taxa, and that observed abrupt changes
704 in these ratios suggest co-existence of several SAR11 strains with different life strategies and
705 phage susceptibility (122). Phenotypic stochasticity of phage receptor expression has been
706 shown to maintain a small proportion of phage-insensitive hosts within a population, enabling
707 coexistence of predator and prey without extinction (123). Phages adsorb to a vast array of
708 receptor proteins on their hosts, with many well-characterised receptors (e.g. OmpC, TonB,
709 BtuB, LamB) associated with nutrient uptake or osmoregulation (124). Selection therefore
710 favours phenotypes that limit receptor expression, with an associated fitness cost, particularly in
711 nutrient-limited environments. However, an alternative mechanism is possible if a population of
712 cells comprised a small number of viable cells, and a large number of non-viable or dormant
713 cells where metabolism is restricted but presentation of receptor proteins is retained. The
714 majority of host-virus encounters would occur with non-viable cells, and constrain viral
715 propagation through inefficient or failed infection, effectively acting as a sink for infectious
716 particles. Thus, the population as a whole can maintain expression of receptor proteins, while
717 reducing viral predation, with low-viability cells retaining the possibility of a return to normal
718 phenotypic growth if and when viral selection pressure abates. Similar systems of bacterial
719 phenotypic bistability associated with antibiotic tolerance and survival in harsh environments are
720 well documented (125, 126) and have been suggested as a possible mechanism for maintaining
721 long-term co-stability between the abundant phage ϕ CrAss001 and its host in the human gut
722 (127).

723 Detailed measurements of dormancy in SAR11 and what types of cellular functions
724 become inactivated are part of our ongoing work. In the meantime, it is worth it to think about
725 the implications of a substantial proportion of non-dividing cells for our understanding of basic
726 growth dynamics. Studies attempting to measure SAR11 growth rates in nature have yielded a
727 wide range of results, ranging from 0.03-1.8 day⁻¹ (97, 105, 108, 128–130). These span wider
728 growth rates than observed for axenic cultures of SAR11 (0.4-1.2 day⁻¹), but isolate-specific
729 growth ranges within that spread are much more constrained (29, 36, 49, 131, 132)). Conversion
730 factors for determining production from ³H-leucine incorporation appear to be accurate for at
731 least Ia subclade members of SAR11 (133), so variations in growth rate estimates from
732 microradiography experiments likely have other explanations. It is possible that different strains
733 of SAR11 simply have variations in growth rate not captured by existing isolates. Another, not
734 mutually exclusive, possibility is that the differences in *in situ* growth rate estimates also reflect
735 variations in the proportion of actively dividing cells within the population. A simple model of
736 cell division with binary fission where only a subset of cells divide and non-dividing cells
737 persist, rather than die, can still yield logarithmic growth curves (Fig. S10) like those observed
738 for SAR11 in pure culture (29, 49, 134). However, this means that the division rate for the subset
739 of cells that are actively dividing is much higher than calculated when assuming 100% viability
740 in the population. Based on our estimated viability for SAR11 LD12 of 15-55%, to obtain our
741 previously calculated maximum division rate (0.5 day⁻¹) for the whole culture (29), the per-cell
742 division rate for only a subpopulation would span 2.48-0.79 day⁻¹ (Fig. S10, Supplemental Text).
743 Verifying the proportion of SAR11 cells actively dividing in a culture may be challenging. Time-

744 lapse microscopy (135) offers an elegant solution if SAR11 can be maintained for the requisite
745 time periods for accurate measurements in a microfluidic device.

746 In addition to identifying taxa whose isolation success suggested deviations from
747 biological assumptions of single planktonic cells with 100% viability, the model also revealed
748 the limitations of DTE cultivation in assessing viability depending on relative abundance (Fig.
749 S9). We cannot ascertain whether any given taxon may violate an assumption of $V = 100\%$
750 unless we have enough wells to demonstrate that it grew in fewer wells than expected. For
751 example, taxa at 1% of the microbial community require more than 1,000 wells before the lack
752 of a cultured organism represents a statistically important negative event, rather than a taxon
753 simply lacking sufficient abundance to ensure inclusion in a well within 95% CI. In our 460 well
754 experiments, we could not resolve whether taxa may have had viabilities below 100% if they
755 were less than 3% of the community for any given experiment (Fig. S9). Modeling DTE
756 experiments showed that for experiments targeting rare taxa, lower inoculum sizes are favoured
757 where selective media for enrichment is either unknown or undesirable. The exponential increase
758 in the number of required wells with respect to the inoculum size is a function of a pure well
759 requiring *all* cells within it to belong to the same taxon, assuming all cells are equally and
760 optimally viable.

761 By providing taxon-specific predictions of viability from cultivation data, our model now
762 facilitates an iterative process to improve experimental design and make cultivation more
763 reliable. First, we use the cultivation success rates to determine for which taxa the assumption of
764 100% viability was violated. Second, we use the model to estimate viability for those organisms.
765 Third, we use the viability and relative abundance data to determine, within 95% CI, the
766 appropriate number of inoculation attempts required to isolate a new version of that organism.
767 Using SAR11 LD12 as an example, given a relative abundance of 10%, and a viability of 15%,
768 800 DTE wells should yield four pure, positive wells (1-8 95% CI). This means that, for
769 microorganisms that we know successfully grow in our media, we can now statistically constrain
770 the appropriate number of wells required to culture a given taxon again. For organisms that were
771 not abundant enough to estimate viability using the model, we can use a conservative viability
772 assumption (e.g., 50% (111)) with which to base our cultivation strategy, thereby still reducing
773 uncertainty about the experimental effort necessary to re-isolate one of these microorganisms.

774 775 *Conclusions*

776 This work has provided hundreds of new cultures for microbiological research, many among the
777 most abundant members of the nGOM coastal bacterioplankton community. It also provides
778 another demonstration of the effectiveness of sustained cultivation efforts for bringing previously
779 uncultivated strains into culture. Our modeled cultivation results have generated compelling
780 evidence for low viability within subpopulations of SAR11 LD12 and IIIa.1, as well as OM43
781 *Betaproteobacteria*. The prevalence of, and controls on, dormancy in these clades deserves
782 further study. We anticipate that future work with larger DTE experiments will yield similar
783 viability data about other groups of taxa with lower abundance, highlighting a valuable
784 diagnostic application of DTE cultivation/modeling beyond the primary role in isolating new
785 microorganisms. The integration of cultivation results, natural abundance data from inoculum
786 communities, and DTE modeling represents an important step forward in quantifying the risk
787 associated with DTE efforts to isolate valuable taxa from new sources, or repeating isolation
788 from the same locations. We hope variations of this approach will be incorporated into wider
789 community efforts to invest in culturing the uncultured.

790
791
792
793
794
795
796
797
798
799
800
801
802
803
804
805
806
807
808
809
810
811
812
813
814
815
816
817
818
819
820
821

Acknowledgments

We would like to thank Dr. Nancy Rabalais for her comments and edits on a very early draft of this manuscript. Portions of this research were conducted with high-performance computing resources provided by Louisiana State University (<http://www.hpc.lsu.edu>) and the University of Southern California (<http://hpc.usc.edu>).

Funding Information

This work was supported by the Department of Biological Sciences at Louisiana State University, a Louisiana Board of Regents grant to JCT (LEQSF(2014-17)-RD-A-06), a National Academies of Science, Engineering, and Medicine Gulf Research Program Early Career Fellowship to JCT, and the Dornsife College of Letters, Arts and Sciences at the University of Southern California. BT was partially funded by NERC award NE/R010935/1 and by the Simons Foundation BIOS-SCOPE program. The funders had no role in study design, data collection, and interpretation, or the decision to submit the work for publication.

Author Contributions

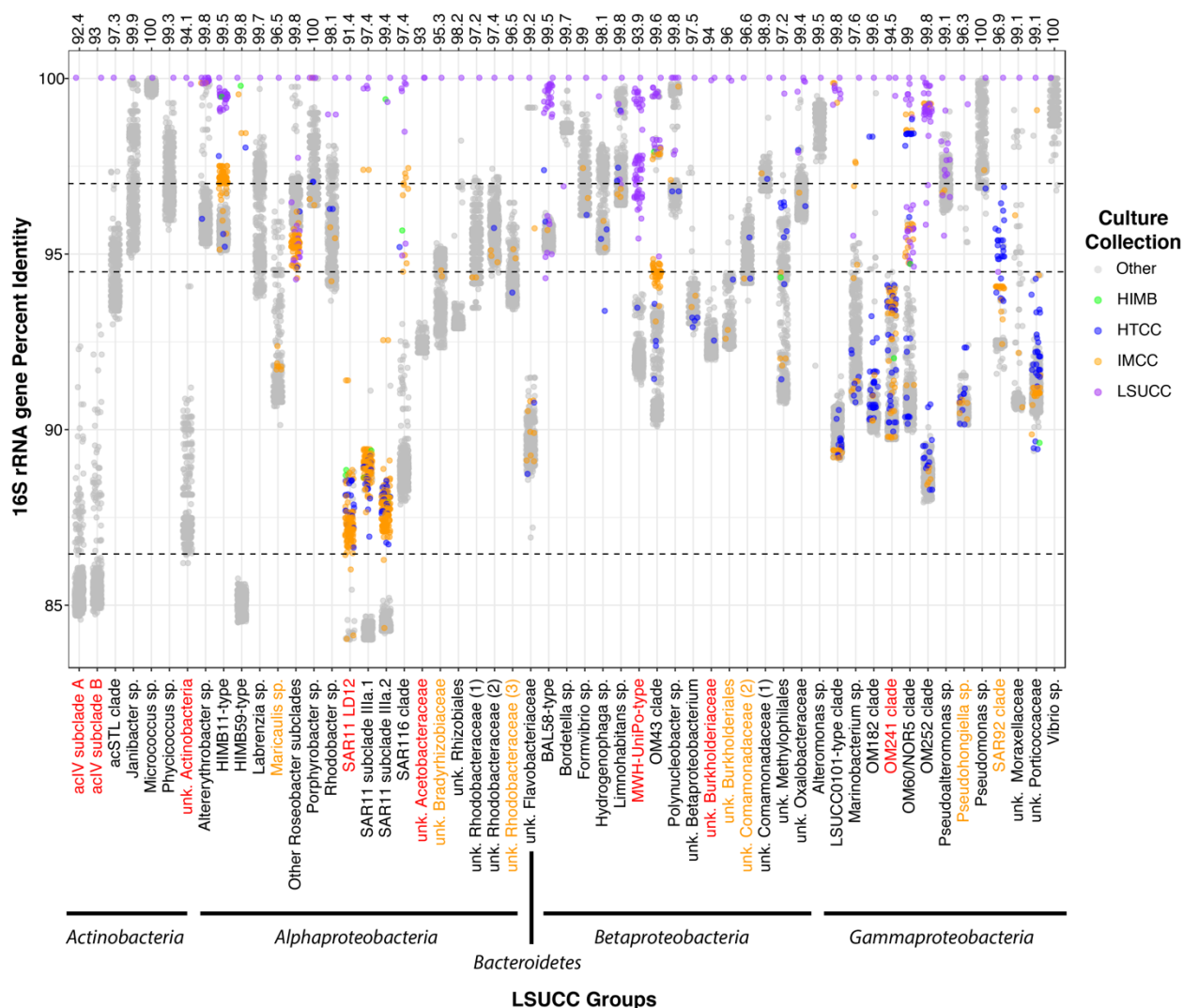
MWH led sample collections, cultivation experiments, nucleic acid extraction, amplicon sequencing, and analyses; VCL, DMP, JLW, and AML supported sample collections, cultivation experiments, and nucleic acid extractions; MWH and JCT conducted cultivation comparisons and phylogenetic analyses; BT developed the viability model and led the statistical analyses; CC derived the cell-specific growth rate equations incorporating viability; JCT designed the study and assisted with sample collections and model refinement; MWH, BT, and JCT led manuscript writing; and all authors contributed to and reviewed the text.

822 **Figures**

823

824

825



826

827

828 **Figure 1.** Percent identity of LSUCC isolate 16S rRNA genes compared with those from other
 829 isolates in NCBI (“Other”, gray dots) or from the DTE culture collections IMCC (gold dots),
 830 HTCC (blue dots), and HIMB (green dots). Each dot represents a pairwise 16S rRNA gene
 831 comparison (via BLASTn). X-axis categories are groups designated according to $\geq 94\%$
 832 sequence identity and phylogenetic placement (see Figs S1-S4). Above the graph is the 16S
 833 rRNA gene sequence percent identity to the closest non-LSUCC isolate within a column. Groups
 834 colored in red indicate those where LSUCC isolates represent putatively novel genera, whereas
 835 orange indicates putatively novel species.

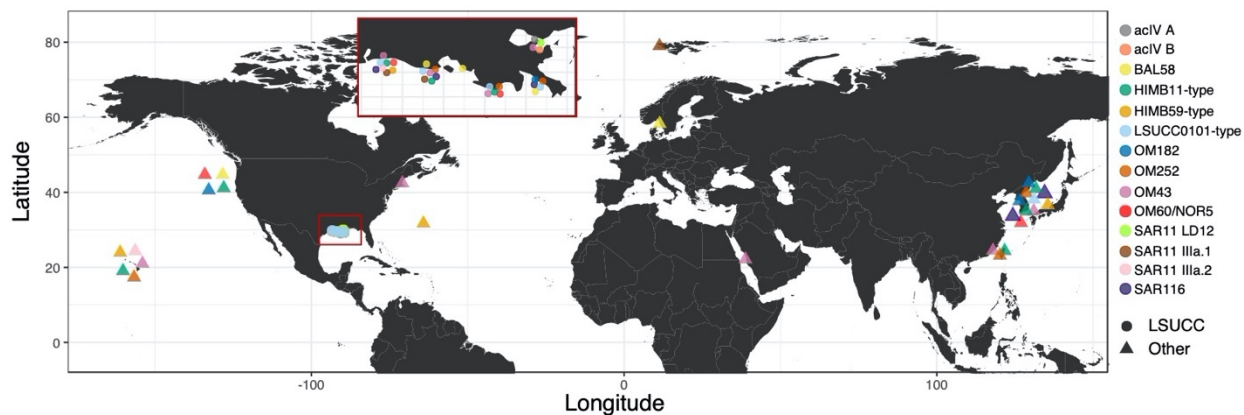
836

837

838

839

840
841
842
843
844
845

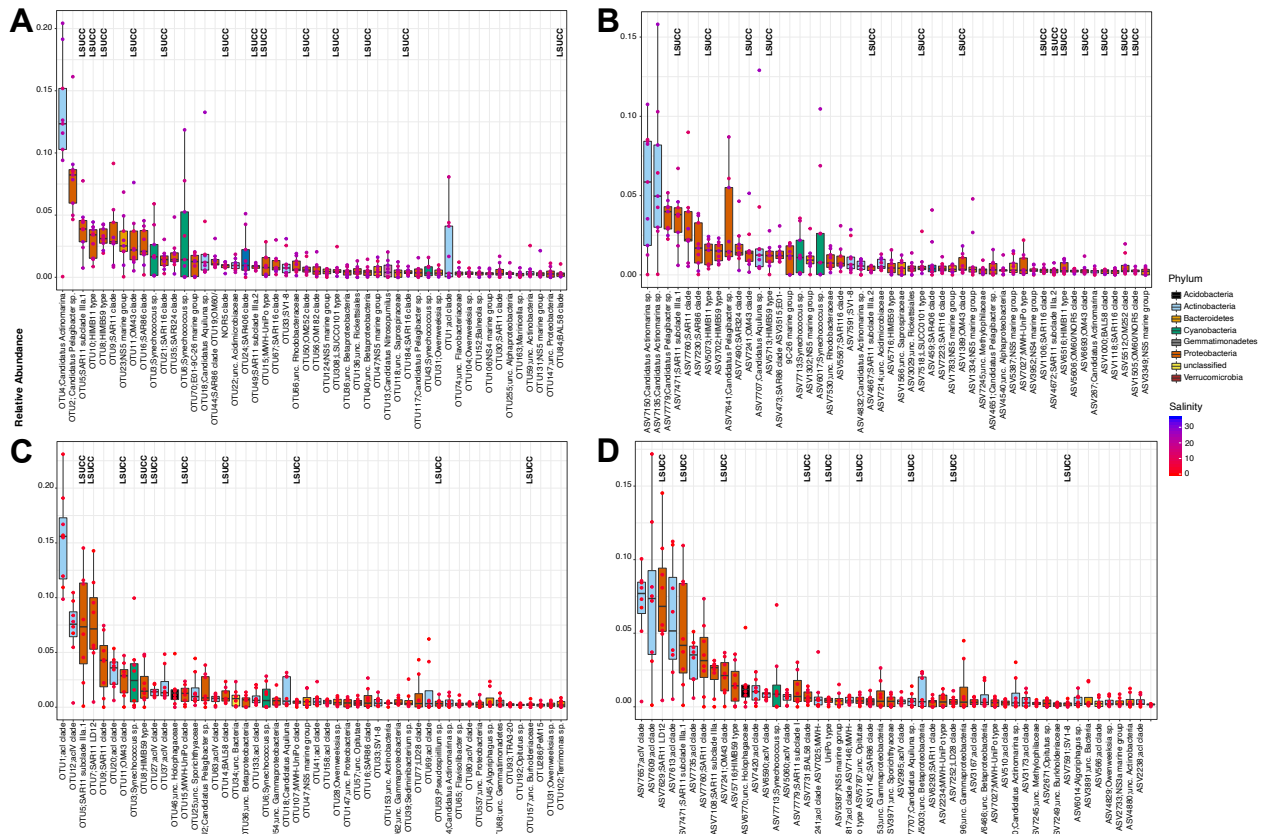


846
847

Figure 2. A global map of the isolation location of isolates from selected important aquatic bacterioplankton clades. Circles represent LSUCC isolates, while triangles are non-LSUCC isolates. Inset: a zoomed view of the coastal Louisiana region where LSUCC bacterioplankton originated.

851
852
853
854
855
856
857
858
859
860
861
862
863
864
865
866
867
868
869
870
871
872
873
874
875

876
877

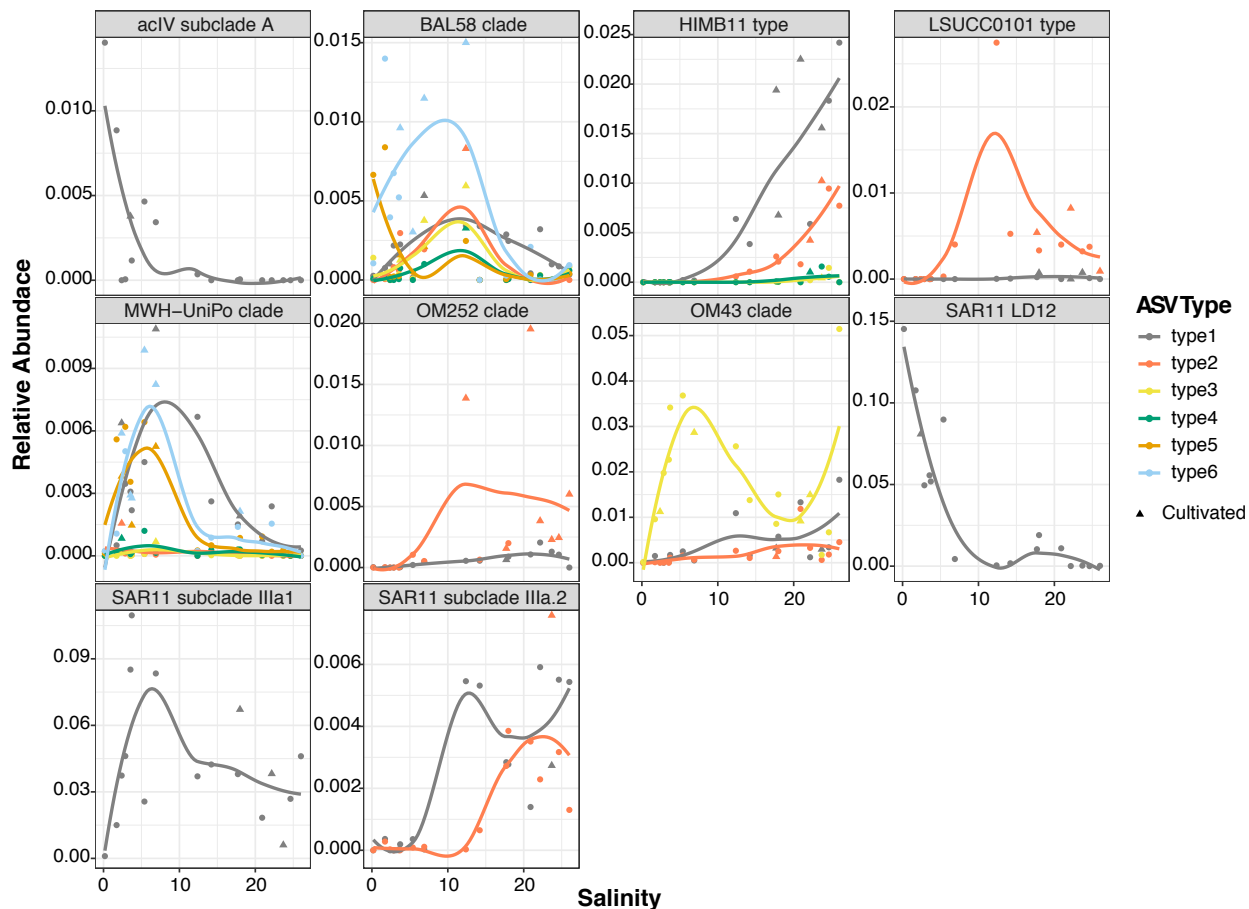


878
879
880

881 **Figure 3.** Rank abundances of the 50 most abundant taxa based on median relative abundance at
882 salinities less than seven (top) and greater than twelve (bottom) for OTUs (A, C) and ASVs (B,
883 D) across all sites. The boxes indicate the interquartile range (IQR) of the data, with vertical lines
884 indicating the upper and lower extremes according to 1.5 x IQR. Horizontal lines within each
885 box indicate the median. The data points comprising the distribution are plotted on top of the
886 boxplots. The shade of the dot represents the salinity at the sample site (red-blue :: lower-higher),
887 while the color of the box indicates broad taxonomic identity. LSUCC labels indicate OTUs and
888 ASVs with at least one cultivated representative.

889
890
891
892
893
894
895
896
897
898
899

900
901
902

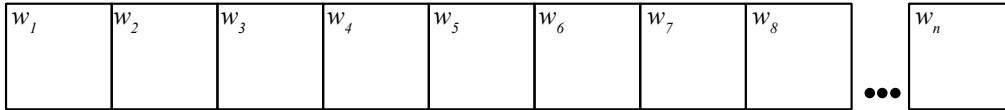


903
904
905
906
907
908
909
910
911
912
913
914
915
916
917
918
919
920
921
922

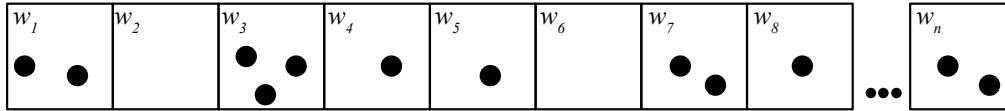
Figure 4. Relative abundance of ASVs within key taxonomic groups compared with salinity. ASV types are colored independently, and triangle points indicate experiments for which at least one isolate was obtained. Non-linear regression lines are provided as a visual aid for abundance trends.

923
924
925

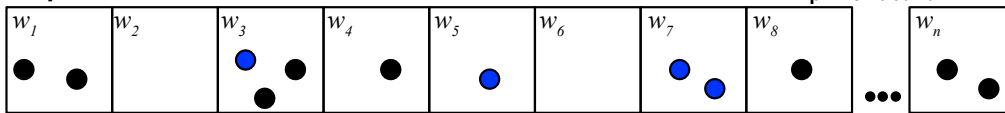
Step 1: Simulate n wells



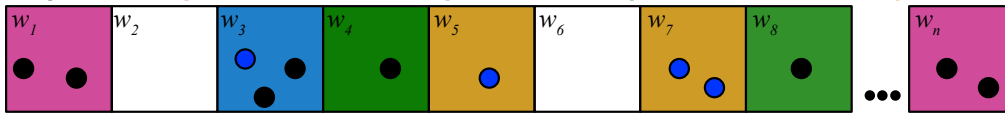
Step 2: Simulate inoculation of wells from Poisson distribution (λ =inoculum)



Step 3: Simulate likelihood of taxon from Binomial distribution (n = # cells in well, p = rel. abund)



Step 4: Count positive wells, taxon positive wells, pure wells and taxon pure wells

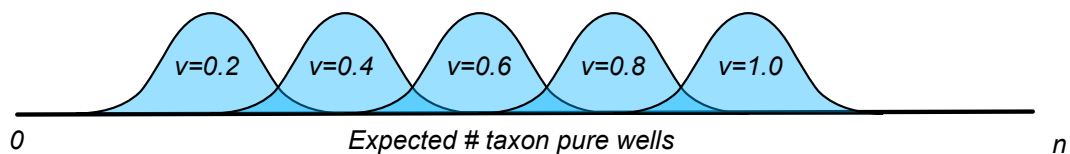


Step 5: For taxon pure wells, simulate likelihood of viability from Binomial distribution (n = # cells in well, p = viability)

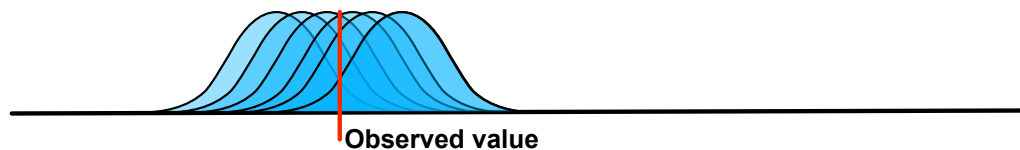


Step 6: Count wells where viable cells ≥ 1

Step 7: Bootstrap steps 1-6 k times at different levels of viability, $0 \leq v \leq 1$



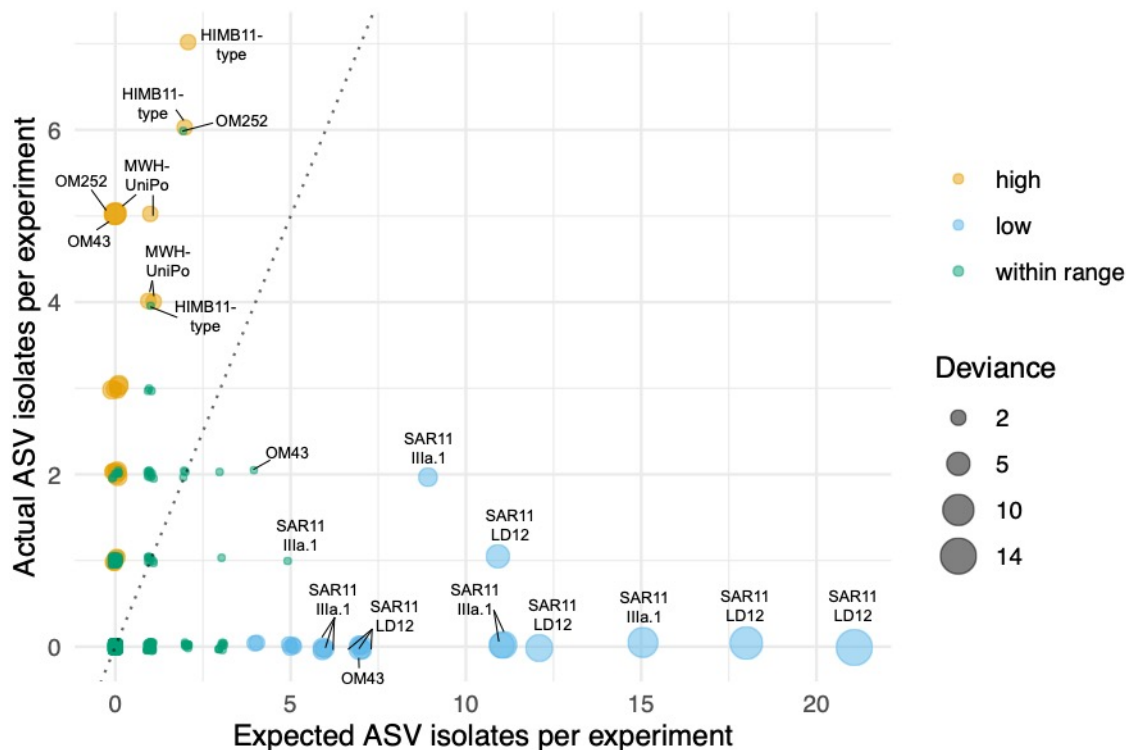
Step 8: Identify min, max values of v where # observed wells falls within bootstrapped 95% CI



926
927
928
929
930

Figure 5. Graphical depiction of the viability model.

931
932
933
934
935



936
937
938
939
940
941
942
943
944
945
946
947
948
949
950
951
952
953

Figure 6. Actual vs. expected numbers of isolates. Each point represents the actual number of isolates for every ASV/experiment pair compared to the expected number of isolates based on our model assuming 100% viability. Colors represent the relationship to the model predictions: green- relative abundance low enough whereby 0 isolates fell within the 95% CI; pink- isolation results within the 95% CI for taxa with relative abundance $\geq 2.9\%$; orange- actual isolates $>$ maximum 95% CI for expected isolates; blue- actual isolates $<$ minimum 95% CI for expected isolates. Circle size is proportional to the deviation of the number of actual isolates from the maximum (for orange) or minimum (for blue) 95% CI for expected isolates. The dotted line is the 1:1 ratio. Notable taxa on the extremities of the actual and expected values are labeled.

954 **Supplemental Information**

955

956 **Supplemental Text**

957 Math for back calculating the per-cell division rates in Henson et al. 2018 assuming 15%--55%
958 viability.

959

960 Denote the initial cell count as X_0 , and the cell count in n^{th} generation as X_n . If all the cells are
961 viable, per each generation, all the cells are doubling:

962

963
$$X_n = X_{n-1} \cdot 2 \quad (\text{eq. S1.1})$$

964

965 And therefore, after n generations, the cell count X_n would be:

966
$$X_n = X_0 \cdot 2^n \quad (\text{eq. S1.2})$$

967

968 When not all the cells are viable, for each generation, instead of simply doubling the whole
969 population, only a portion of the cells (denoted as $V < 1$) replicates. In this case:

970

971
$$X_n = X_{n-1} \cdot (1 + V) \quad (\text{eq. S1.3})$$

972

973 Here we can see that (eq. 3.1) is actually a special case of (eq. 3.3), when $V = 1$,

974

975
$$X_n = X_{n-1} \cdot (1 + 1) = X_{n-1} \cdot 2$$

976

977 When $V < 1$, after n generations:

978
$$X_n = X_0 \cdot (1 + V)^n \quad (\text{eq. S1.4})$$

979

980 Denoting the total time to get n generations as t , which means the number of generations per unit
981 time, also known as the per-cell division rate, is $\mu = n/t$. Rewriting (eq. 3.4), we have:

982

983
$$X_n = X_0 \cdot (1 + V)^{\mu \cdot t} = X_0 \cdot 2^{\mu \cdot \log_2(1+V) \cdot t} \quad (\text{eq. S1.5})$$

984

985 According to (eq. 3.5), a cell population of V viability and μ per cell division rate, the population
986 division rate is:

987
$$\mu_{population} = \mu \cdot \log_2(1 + V) \quad (\text{eq. S1.6})$$

988

989 Henson et al. 2018 show that the optimal population division rate of SAR11 LD12 is

990 $\mu_{population} = 0.5 \text{ day}^{-1}$, assuming the viability of LD12 is $V = 0.15$, by plugging in these two
991 numbers to (eq. S1.6), we can get the per-cell division rate of LD12 is:

992

993
$$\begin{aligned} \mu &= \mu_{population} / \log_2(1 + V) \\ &= 0.5 \text{ day}^{-1} / \log_2(1 + 0.15) \\ &= 0.5 \text{ day}^{-1} / 0.20163 \\ &= 2.48 \text{ day}^{-1} \end{aligned}$$

994

995 If assuming $V = 0.55$, $\mu = 0.79 \text{ day}^{-1}$. Therefore, given the range of the viability of LD12 is
997 between 15%--55%, the corresponding per cell division rate is between 0.79 divisions to 2.48
998 divisions per day.

999
1000
1001
1002
1003
1004
1005
1006
1007
1008
1009
1010
1011
1012
1013
1014
1015
1016
1017
1018
1019
1020
1021
1022
1023
1024
1025
1026
1027
1028
1029
1030
1031
1032
1033
1034
1035
1036
1037
1038
1039
1040
1041
1042
1043
1044

Supplemental Table

Supplemental Table S1 is a spreadsheet, Table_S1.xlsx. This includes MWH media recipes, ASV and OTU tables, taxonomic and relative abundance information for all isolates, NMDS information, biogeochemical data for the samples, and the BLAST results of isolate hits. Available at <https://doi.org/10.6084/m9.figshare.12142113>.

Supplemental Figures

Figure S1. 16S rRNA gene phylogeny of LSUCC isolates in the Phylum *Actinobacteria*. Scale bar represents 0.01 changes per position. Values at internal nodes indicate bootstrap values (n = 1000).

Figure S2. 16S rRNA gene phylogeny of LSUCC isolates in the Class *Alphaproteobacteria*. Scale bar represents 0.01 changes per position. Values at internal nodes indicate bootstrap values (n = 1000).

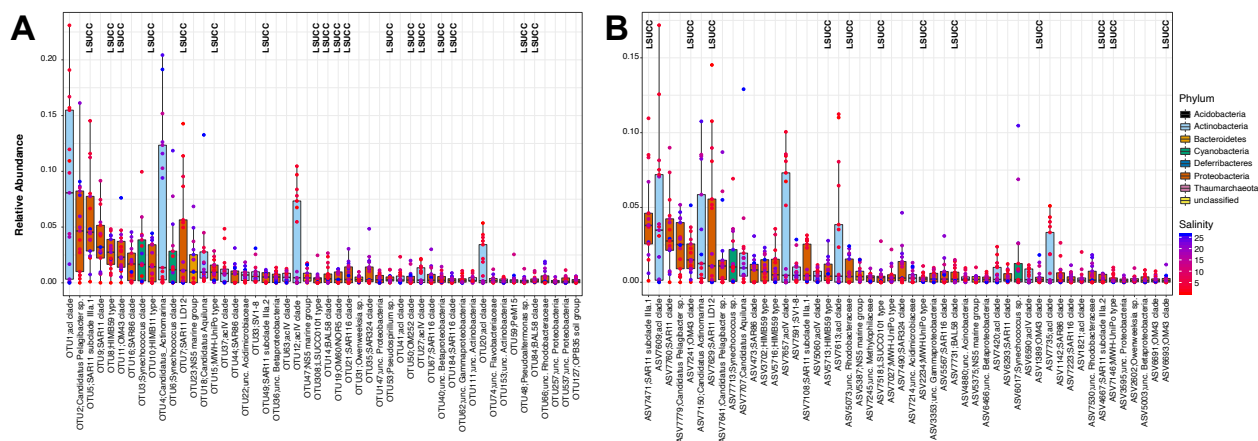
Figure S3. 16S rRNA gene phylogeny of LSUCC isolates in the Phylum *Bacteroidetes*. Scale bar represents 0.01 changes per position. Values at internal nodes indicate bootstrap values (n = 1000).

Figure S4. 16S rRNA gene phylogeny of LSUCC isolates in the Class *Betaproteobacteria*. Scale bar represents 0.01 changes per position. Values at internal nodes indicate bootstrap values (n = 1000).

Figure S5. 16S rRNA gene phylogeny of LSUCC isolates in the Class *Gammaproteobacteria*. Scale bar represents 0.01 changes per position. Values at internal nodes indicate bootstrap values (n = 1000).

These trees have been attached at the end of the manuscript for greater visibility

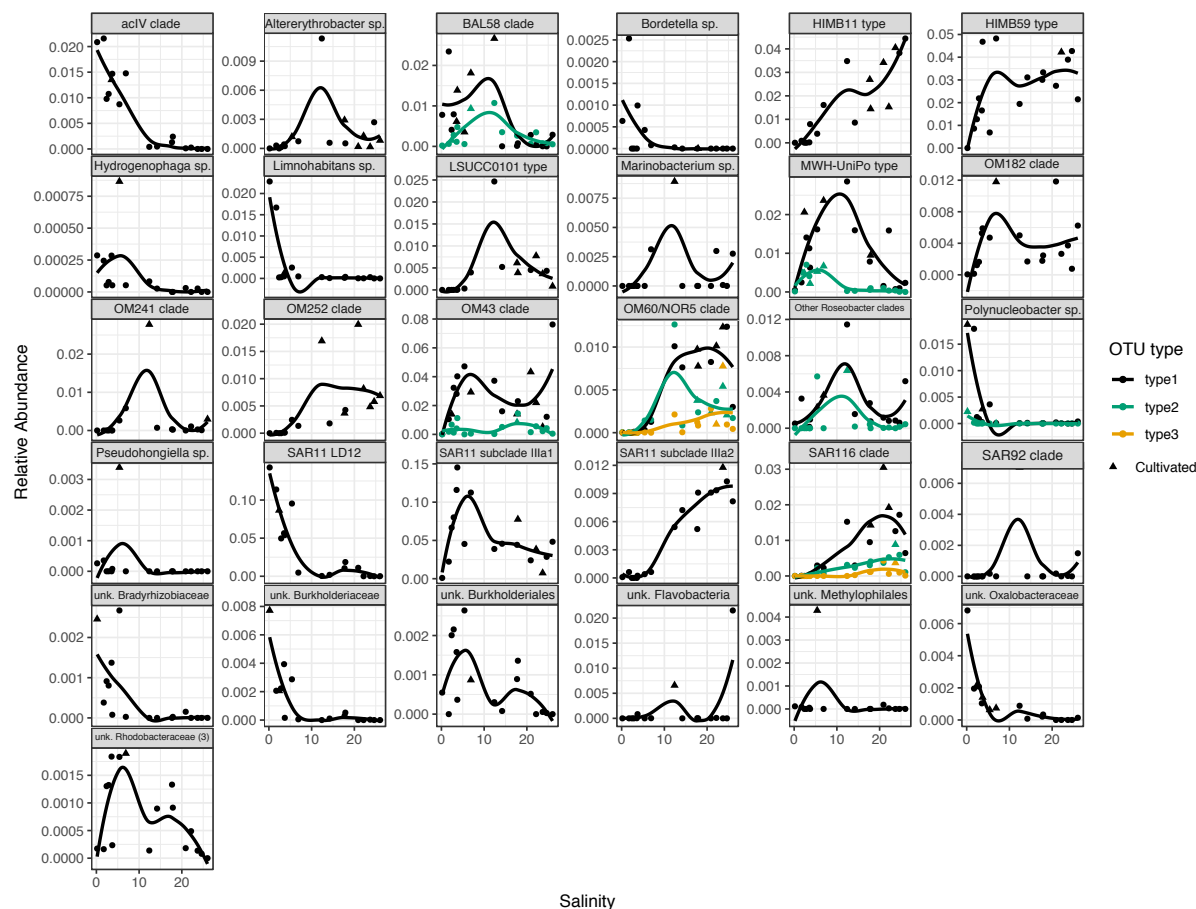
1045
1046
1047
1048



1049
1050
1051
1052
1053
1054
1055
1056
1057
1058
1059
1060
1061
1062
1063
1064
1065
1066
1067
1068
1069
1070
1071
1072
1073
1074
1075
1076
1077
1078
1079
1080

Figure S6. Rank abundance plot of the top 50 most abundant (A) OTUs and (B) ASVs across all sites. The boxes indicate the interquartile range (IQR) of the data, with vertical lines indicating the upper and lower extremes according to 1.5 x IQR. Horizontal lines within each box indicate the median. The underlying data points are each individual OTU's sample relative abundances. The shade of the dot represents the salinity, while the color of the box is the Phylum of the OTU. OTUs with cultured representatives from the LSU culture collection are labeled with one LSUCC isolate.

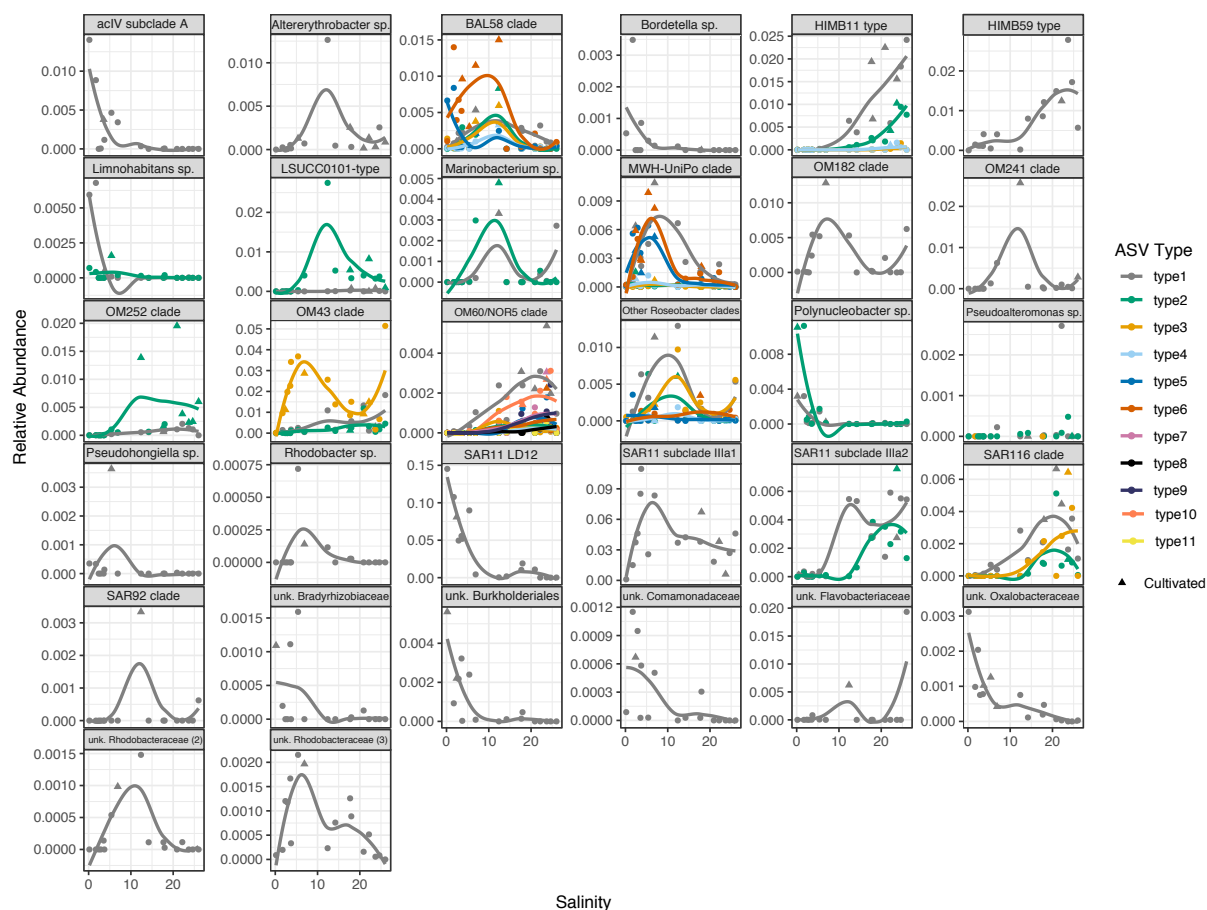
1081
1082
1083
1084
1085
1086



1087
1088
1089
1090
1091
1092
1093
1094
1095
1096
1097
1098
1099
1100
1101
1102
1103

Figure S7. Relative abundance of cultivated OTUs according to site salinity. The color of the line represents the different OTUs classified within the LSUCC group. Non-linear regressions have been added for reference.

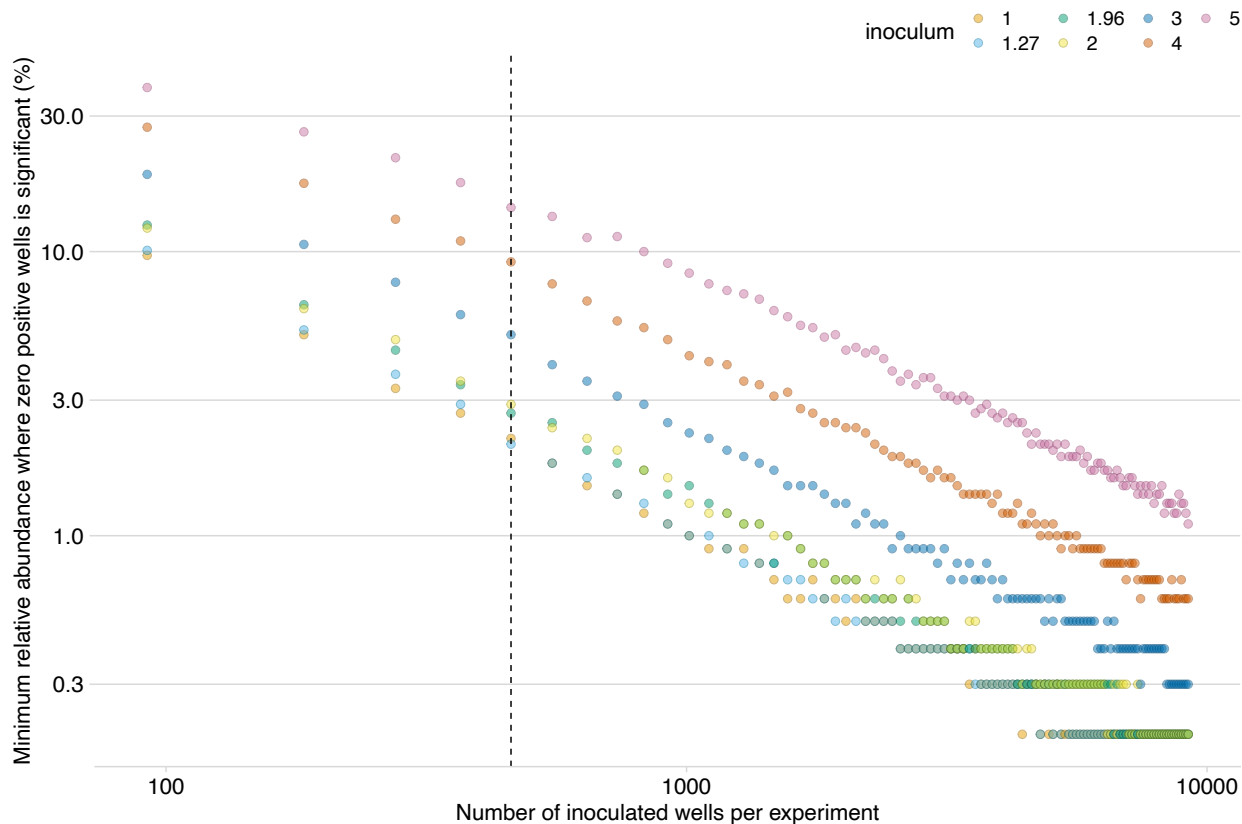
1104
1105
1106
1107



1108
1109
1110
1111
1112
1113
1114
1115
1116
1117
1118
1119
1120
1121
1122
1123
1124
1125
1126

Figure S8. Relative abundance of ASVs with a cultured LSUCC representative according to site salinity. The color of the line represents the different ASVs classified within the LSUCC group. Non-linear regressions have been added for reference. Arrows represent sites where isolates were cultivated.

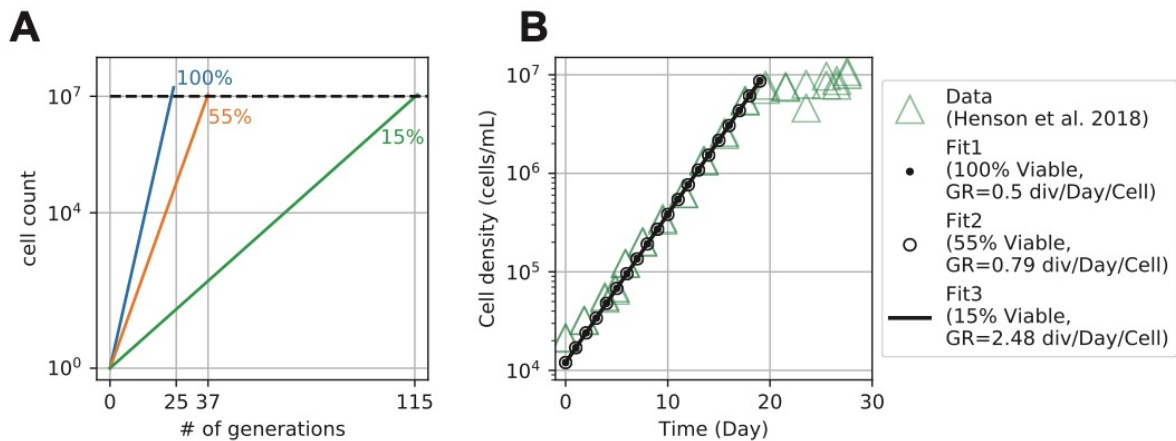
1127
1128
1129
1130
1131



1132
1133
1134
1135
1136
1137
1138
1139
1140
1141
1142
1143
1144
1145
1146
1147
1148
1149
1150
1151

Figure S9. Sensitivity testing of the viability model to determine minimum numbers of wells required to overcome false negatives associated with differing levels of taxon relative abundance. Different inoculum densities (λ) are depicted with colors. The dotted line indicates 460 wells which corresponded to the experiments in this study.

1152
1153
1154
1155
1156
1157
1158
1159



1160
1161
1162
1163
1164
1165
1166
1167
1168
1169
1170
1171
1172
1173
1174
1175

Figure S10. Logarithmic growth with different percentages of cell viability. Under different cell viabilities, such as 100%, 55% and 15% shown in (A), the culture can have logarithmic growth in the population size if we assume no cell death. It takes around 25 generations to have 10^7 fold expansion of population size when all cells are active (100% viable), whereas when 15% of the population is actively duplicating, it takes around 115 generations to reach the same population size expansion. B) For the SAR11 LD12 strain LSUCC0530, the previously measured population doubling rate was 0.5/day (29). If all the cells are active (100% viability), each cell within the population will double 0.5 times per day (Fit 1 in B). However, with 15% viability, the actual active cell doubling rate is 2.48 doublings day⁻¹ (Fit 3 in B).

1176 References

- 1177 1. Metcalf WW, Griffin BM, Cicchillo RM, Gao J, Janga SC, Cooke HA, Circello BT, Evans
1178 BS, Martens-Habbena W, Stahl DA, van der Donk WA. 2012. Synthesis of
1179 methylphosphonic acid by marine microbes: a source for methane in the aerobic ocean.
1180 *Science* 337:1104–1107.
- 1181 2. Carini P, White AE, Campbell EO, Giovannoni SJ. 2014. Methane production by
1182 phosphate-starved SAR11 chemoheterotrophic marine bacteria. *Nat Commun* 5:4346.
- 1183 3. Karl DM, Beversdorf L, Björkman KM, Church MJ, Martinez A, Delong EF. 2008. Aerobic
1184 production of methane in the sea. *Nat Geosci* 1:473–478.
- 1185 4. Steindler L, Schwalbach MS, Smith DP, Chan F, Giovannoni SJ. 2011. Energy starved
1186 *Candidatus Pelagibacter ubique* substitutes light-mediated ATP production for endogenous
1187 carbon respiration. *PLoS One* 6:e19725.
- 1188 5. Gómez-Consarnau L, González JM, Coll-Lladó M, Gourdon P, Pascher T, Neutze R,
1189 Pedrós-Alió C, Pinhassi J. 2007. Light stimulates growth of proteorhodopsin-containing
1190 marine Flavobacteria. *Nature* 445:210–213.
- 1191 6. Daims H, Lebedeva EV, Pjevac P, Han P, Herbold C, Albertsen M, Jehmlich N, Palatinszky
1192 M, Vierheilig J, Bulaev A, Kirkegaard RH, von Bergen M, Rattei T, Bendinger B, Nielsen
1193 PH, Wagner M. 2015. Complete nitrification by *Nitrospira* bacteria. *Nature* 528:504–509.
- 1194 7. Lam KS. 2006. Discovery of novel metabolites from marine actinomycetes. *Curr Opin*
1195 *Microbiol* 9:245–251.
- 1196 8. Jensen PR, Williams PG, Oh D-C, Zeigler L, Fenical W. 2007. Species-specific secondary
1197 metabolite production in marine actinomycetes of the genus *Salinispora*. *Appl Environ*
1198 *Microbiol* 73:1146–1152.
- 1199 9. Nett M, Erol Ö, Kehraus S, Köck M, Krick A, Eguereva E, Neu E, König GM. 2006.
1200 Siphonazole, an Unusual Metabolite from *Herpetosiphon* sp. *Angew Chem Int Ed* 45:3863–
1201 3867.
- 1202 10. Ling LL, Schneider T, Peoples AJ, Spoering AL, Engels I, Conlon BP, Mueller A,
1203 Schäberle TF, Hughes DE, Epstein S, Jones M, Lazarides L, Steadman VA, Cohen DR,
1204 Felix CR, Fetterman KA, Millett WP, Nitti AG, Zullo AM, Chen C, Lewis K. 2015. A new
1205 antibiotic kills pathogens without detectable resistance. *Nature* 517:455–459.
- 1206 11. Lloyd KG, Steen AD, Ladau J, Yin J, Crosby L. 2018. Phylogenetically Novel Uncultured
1207 Microbial Cells Dominate Earth Microbiomes. *mSystems* 3:e00055–18.
- 1208 12. Hug LA. 2018. Sizing Up the Uncultured Microbial Majority. *mSystems* 3:e00185–18.
- 1209 13. Steen AD, Crits-Christoph A, Carini P, DeAngelis KM, Fierer N, Lloyd KG, Thrash JC.
1210 2019. High proportions of bacteria and archaea across most biomes remain uncultured.

- 1211 ISME J 13:3126–3130.
- 1212 14. Overmann J, Abt B, Sikorski J. 2017. Present and Future of Culturing Bacteria. *Annu Rev*
1213 *Microbiol* 71:711–730.
- 1214 15. Rappé MS. 2013. Stabilizing the foundation of the house that 'omics builds: the evolving
1215 value of cultured isolates to marine microbiology. *Curr Opin Microbiol* 16:618–624.
- 1216 16. Carini P. 2019. A “Cultural” Renaissance: Genomics Breathes New Life into an Old Craft.
1217 *mSystems* 4:e00092–19.
- 1218 17. Staley JT, Konopka A. 1985. Measurement of in situ activities of nonphotosynthetic
1219 microorganisms in aquatic and terrestrial habitats. *Annu Rev Microbiol* 39:321–346.
- 1220 18. Amann RI, Ludwig W, Schleifer KH. 1995. Phylogenetic identification and in situ detection
1221 of individual microbial cells without cultivation. *Microbiol Rev* 59:143–169.
- 1222 19. Hahn MW, Koll U, Schmidt J. 2019. Isolation and Cultivation of Bacteria, p. 313–351. *In*
1223 Hurst, CJ (ed.), *The Structure and Function of Aquatic Microbial Communities*. Springer
1224 International Publishing, Cham.
- 1225 20. Kaeberlein T, Lewis K, Epstein SS. 2002. Isolating “uncultivable” microorganisms in pure
1226 culture in a simulated natural environment. *Science* 296:1127–1129.
- 1227 21. Zengler K, Toledo G, Rappe M, Elkins J, Mathur EJ, Short JM, Keller M. 2002. Cultivating
1228 the uncultured. *Proc Natl Acad Sci U S A* 99:15681–15686.
- 1229 22. Steinert G, Whitfield S, Taylor MW, Thoms C, Schupp PJ. 2014. Application of Diffusion
1230 Growth Chambers for the Cultivation of Marine Sponge-Associated Bacteria. *Mar*
1231 *Biotechnol* 16:594–603.
- 1232 23. Nichols D, Cahoon N, Trakhtenberg EM, Pham L, Mehta A, Belanger A, Kanigan T, Lewis
1233 K, Epstein SS. 2010. Use of Ichip for High-Throughput In Situ Cultivation of
1234 “Uncultivable” Microbial Species. *Appl Environ Microbiol* 76:2445–2450.
- 1235 24. Tandogan N, Abadian PN, Epstein S, Aoi Y, Goluch ED. 2014. Isolation of microorganisms
1236 using sub-micrometer constrictions. *PLoS One* 9:e101429.
- 1237 25. Hahn MW, Stadler P, Wu QL, Pöckl M. 2004. The filtration–acclimatization method for
1238 isolation of an important fraction of the not readily cultivable bacteria. *J Microbiol Methods*
1239 57:379–390.
- 1240 26. Cannon SA, Giovannoni SJ. 2002. High-throughput methods for culturing microorganisms
1241 in very-low-nutrient media yield diverse new marine isolates. *Appl Environ Microbiol*
1242 68:3878–3885.
- 1243 27. Yang SJ, Kang I, Cho JC. 2016. Expansion of Cultured Bacterial Diversity by Large-Scale
1244 Dilution-to-Extinction Culturing from a Single Seawater Sample. *Microb Ecol* 71:29–43.

- 1245 28. Stingl U, Tripp HJ, Giovannoni SJ. 2007. Improvements of high-throughput culturing
1246 yielded novel SAR11 strains and other abundant marine bacteria from the Oregon coast and
1247 the Bermuda Atlantic Time Series study site. *ISME J* 1:361–371.
- 1248 29. Henson MW, Lanclos VC, Faircloth BC, Thrash JC. 2018. Cultivation and genomics of the
1249 first freshwater SAR11 (LD12) isolate. *ISME J* 12:1846–1860.
- 1250 30. Hahnke RL, Bennke CM, Fuchs BM, Mann AJ, Rhiel E, Teeling H, Amann R, Harder J.
1251 2015. Dilution cultivation of marine heterotrophic bacteria abundant after a spring
1252 phytoplankton bloom in the North Sea. *Environ Microbiol* 17:3515–3526.
- 1253 31. Sosa OA, Gifford SM, Repeta DJ, DeLong EF. 2015. High molecular weight dissolved
1254 organic matter enrichment selects for methylotrophs in dilution to extinction cultures. *ISME*
1255 *J* 9:2725–2739.
- 1256 32. Schut F, de Vries EJ, Gottschal JC, Robertson BR, Harder W, Prins RA, Button DK. 1993.
1257 Isolation of Typical Marine Bacteria by Dilution Culture: Growth, Maintenance, and
1258 Characteristics of Isolates under Laboratory Conditions. *Appl Environ Microbiol* 59:2150–
1259 2160.
- 1260 33. Button DK, Schut F, Quang P, Martin R, Robertson BR. 1993. Viability and isolation of
1261 marine bacteria by dilution culture: theory, procedures, and initial results. *Appl Environ*
1262 *Microbiol* 59:881–891.
- 1263 34. Song J, Oh HM, Cho JC. 2009. Improved culturability of SAR11 strains in dilution-to-
1264 extinction culturing from the East Sea, West Pacific Ocean. *FEMS Microbiol Lett* 295:141–
1265 147.
- 1266 35. Henson MW, Pitre DM, Weckhorst JL, Lanclos VC, Webber AT, Thrash JC. 2016.
1267 Artificial Seawater Media Facilitate Cultivating Members of the Microbial Majority from
1268 the Gulf of Mexico. *mSphere* 1:e00028–16.
- 1269 36. Rappé MS, Connon SA, Vergin KL, Giovannoni SJ. 2002. Cultivation of the ubiquitous
1270 SAR11 marine bacterioplankton clade. *Nature* 418:630–633.
- 1271 37. Marshall KT, Morris RM. 2013. Isolation of an aerobic sulfur oxidizer from the
1272 SUP05/Arctic96BD-19 clade. *ISME J* 7:452–455.
- 1273 38. Shah V, Chang BX, Morris RM. 2017. Cultivation of a chemoautotroph from the SUP05
1274 clade of marine bacteria that produces nitrite and consumes ammonium. *ISME J* 11:263–
1275 271.
- 1276 39. Spietz RL, Lundeen RA, Zhao X, Nicastro D, Ingalls AE, Morris RM. 2019. Heterotrophic
1277 carbon metabolism and energy acquisition in *Candidatus Thioglobus singularis* strain PS1, a
1278 member of the SUP05 clade of marine Gammaproteobacteria. *Environ Microbiol* 21:2391–
1279 2401.
- 1280 40. Huggett MJ, Hayakawa DH, Rappé MS. 2012. Genome sequence of strain HIMB624, a

- 1281 cultured representative from the OM43 clade of marine Betaproteobacteria. *Stand Genomic*
1282 *Sci* 6:11–20.
- 1283 41. Giovannoni SJ, Hayakawa DH, Tripp HJ, Stingl U, Givan SA, Cho J-C, Oh H-M, Kitner
1284 JB, Vergin KL, Rappé MS. 2008. The small genome of an abundant coastal ocean
1285 methyloph. *Environ Microbiol* 10:1771–1782.
- 1286 42. Durham BP, Grote J, Whittaker KA, Bender SJ, Luo H, Grim SL, Brown JM, Casey JR,
1287 Dron A, Florez-Leiva L, Others. 2014. Draft genome sequence of marine
1288 alphaproteobacterial strain HIMB11, the first cultivated representative of a unique lineage
1289 within the Roseobacter clade possessing an unusually small genome. *Stand Genomic Sci*
1290 9:632–645.
- 1291 43. Cho JC, Giovannoni SJ. 2004. Cultivation and Growth Characteristics of a Diverse Group
1292 of Oligotrophic Marine Gammaproteobacteria. *Appl Environ Microbiol* 70:432–440.
- 1293 44. Kim S, Kang I, Seo J-H, Cho J-C. 2019. Culturing the ubiquitous freshwater actinobacterial
1294 acI lineage by supplying a biochemical “helper” catalase. *ISME J* 13:2252–2263.
- 1295 45. Tripp HJ. 2013. The unique metabolism of SAR11 aquatic bacteria. *J Microbiol* 51:147–
1296 153.
- 1297 46. Nichols D, Lewis K, Orjala J, Mo S, Ortenberg R, O’Connor P, Zhao C, Vouros P,
1298 Kaerberlein T, Epstein SS. 2008. Short Peptide Induces an “Uncultivable” Microorganism
1299 To Grow In Vitro. *Appl Environ Microbiol* 74:4889–4897.
- 1300 47. Stewart EJ. 2012. Growing unculturable bacteria. *J Bacteriol* 194:4151–4160.
- 1301 48. Kell DB, Young M. 2000. Bacterial dormancy and culturability: the role of autocrine
1302 growth factors. *Curr Opin Microbiol* 3:238–243.
- 1303 49. Carini P, Steindler L, Beszteri S, Giovannoni SJ. 2013. Nutrient requirements for growth of
1304 the extreme oligotroph “*Candidatus Pelagibacter ubique*” HTCC1062 on a defined medium.
1305 *ISME J* 7:592–602.
- 1306 50. Epstein SS. 2013. The phenomenon of microbial uncultivability. *Curr Opin Microbiol*
1307 16:636–642.
- 1308 51. Shah D, Zhang Z, Khodursky A, Kaldalu N, Kurg K, Lewis K. 2006. Persisters: a distinct
1309 physiological state of *E. coli*. *BMC Microbiol* 6:53.
- 1310 52. Kell D, Potgieter M, Pretorius E. 2015. Individuality, phenotypic differentiation, dormancy
1311 and “persistence” in culturable bacterial systems: commonalities shared by environmental,
1312 laboratory, and clinical microbiology. *F1000Res* 4:179.
- 1313 53. Lennon JT, Jones SE. 2011. Microbial seed banks: the ecological and evolutionary
1314 implications of dormancy. *Nat Rev Microbiol* 9:119–130.

- 1315 54. Grassi L, Di Luca M, Maisetta G, Rinaldi AC, Esin S, Trampuz A, Batoni G. 2017.
1316 Generation of persister cells of *Pseudomonas aeruginosa* and *Staphylococcus aureus* by
1317 chemical treatment and evaluation of their susceptibility to membrane-targeting agents.
1318 *Front Microbiol* 8:1917.
- 1319 55. Bergkessel M, Basta DW, Newman DK. 2016. The physiology of growth arrest: uniting
1320 molecular and environmental microbiology. *Nat Rev Microbiol* 14:549–562.
- 1321 56. Kussell E, Leibler S. 2005. Phenotypic diversity, population growth, and information in
1322 fluctuating environments. *Science* 309:2075–2078.
- 1323 57. Kurm V, van der Putten WH, Gera Hol WH. 2019. Cultivation-success of rare soil bacteria
1324 is not influenced by incubation time and growth medium. *PLoS One* 14:e0210073.
- 1325 58. D’Onofrio A, Crawford JM, Stewart EJ, Witt K, Gavrish E, Epstein S, Clardy J, Lewis K.
1326 2010. Siderophores from neighboring organisms promote the growth of uncultured bacteria.
1327 *Chem Biol* 17:254–264.
- 1328 59. Thrash JC. 2019. Culturing the Uncultured: Risk versus Reward. *mSystems* 4:e00130–19.
- 1329 60. Thrash JC, Weckhorst JL, Pitre DM. 2017. Cultivating Fastidious Microbes, p. 57–78. *In*
1330 McGenity, TJ, Timmis, KN, Nogales, B (eds.), *Hydrocarbon and Lipid Microbiology*
1331 *Protocols*. Springer Berlin Heidelberg, Berlin, Heidelberg.
- 1332 61. Vila-Costa M, Simó R, Harada H, Gasol JM, Slezak D, Kiene RP. 2006.
1333 Dimethylsulfoniopropionate uptake by marine phytoplankton. *Science* 314:652–654.
- 1334 62. Mou X, Hodson RE, Moran MA. 2007. Bacterioplankton assemblages transforming
1335 dissolved organic compounds in coastal seawater. *Environ Microbiol* 9:2025–2037.
- 1336 63. Stein LY. 2015. Microbiology: Cyanate fuels the nitrogen cycle. *Nature* 524:43–44.
- 1337 64. Repeta DJ, Ferrón S, Sosa OA, Johnson CG, Repeta LD, Acker M, Delong EF, Karl DM.
1338 2016. Marine methane paradox explained by bacterial degradation of dissolved organic
1339 matter. *Nat Geosci* 9:884–887.
- 1340 65. Curson ARJ, Liu J, Bermejo Martínez A, Green RT, Chan Y, Carrión O, Williams BT,
1341 Zhang S-H, Yang G-P, Bulman Page PC, Zhang X-H, Todd JD. 2017.
1342 Dimethylsulfoniopropionate biosynthesis in marine bacteria and identification of the key
1343 gene in this process. *Nat Microbiol* 2:17009.
- 1344 66. Widner B, Mulholland MR. 2017. Cyanate distribution and uptake in North Atlantic coastal
1345 waters. *Limnol Oceanogr* 62:2538–2549.
- 1346 67. Widner B, Mulholland MR, Mopper K. 2016. Distribution, Sources, and Sinks of Cyanate
1347 in the Coastal North Atlantic Ocean. *Environ Sci Technol Lett* 3:297–302.
- 1348 68. Henson MW, Hanssen J, Spooner G, Fleming P, Pukonen M, Stahr F, Thrash JC. 2018.

- 1349 Nutrient dynamics and stream order influence microbial community patterns along a 2914
1350 kilometer transect of the Mississippi River. *Limnol Oceanogr* 63:1837–1855.
- 1351 69. Apprill A, McNally S, Parsons R, Weber L. 2015. Minor revision to V4 region SSU rRNA
1352 806R gene primer greatly increases detection of SAR11 bacterioplankton. *Aquat Microb*
1353 *Ecol* 75:129–137.
- 1354 70. Walters W, Hyde ER, Berg-Lyons D, Ackermann G, Humphrey G, Parada A, Gilbert JA,
1355 Jansson JK, Caporaso JG, Fuhrman JA, Apprill A, Knight R. 2016. Improved Bacterial 16S
1356 rRNA Gene (V4 and V4-5) and Fungal Internal Transcribed Spacer Marker Gene Primers
1357 for Microbial Community Surveys. *mSystems* 1:e00009–15.
- 1358 71. Schloss PD, Westcott SL, Ryabin T, Hall JR, Hartmann M, Hollister EB, Lesniewski R a.,
1359 Oakley BB, Parks DH, Robinson CJ, Sahl JW, Stres B, Thallinger GG, Van Horn DJ,
1360 Weber CF. 2009. Introducing mothur: Open-source, platform-independent, community-
1361 supported software for describing and comparing microbial communities. *Appl Environ*
1362 *Microbiol* 75:7537–7541.
- 1363 72. Pruesse E, Quast C, Knittel K, Fuchs BM, Ludwig W, Peplies J, Glockner FO, Glöckner
1364 FO. 2007. SILVA: a comprehensive online resource for quality checked and aligned
1365 ribosomal RNA sequence data compatible with ARB. *Nucleic Acids Res* 35:7188–7196.
- 1366 73. Quast C, Pruesse E, Yilmaz P, Gerken J, Schweer T, Yarza P, Peplies J, Glöckner FO.
1367 2013. The SILVA ribosomal RNA gene database project: Improved data processing and
1368 web-based tools. *Nucleic Acids Res* 41:590–596.
- 1369 74. Eren AM, Borisy GG, Huse SM, Mark Welch JL. 2014. Oligotyping analysis of the human
1370 oral microbiome. *Proc Natl Acad Sci U S A* 111:E2875–84.
- 1371 75. Fujimoto M, Cavaletto J, Liebig JR, McCarthy A, Vanderploeg HA, Deneff VJ. 2016.
1372 Spatiotemporal distribution of bacterioplankton functional groups along a freshwater
1373 estuary to pelagic gradient in Lake Michigan. *J Great Lakes Res* 42:1036–1048.
- 1374 76. Cole JR, Wang Q, Fish JA, Chai B, McGarrell DM, Sun Y, Brown CT, Porras-Alfaro A,
1375 Kuske CR, Tiedje JM. 2014. Ribosomal Database Project: data and tools for high
1376 throughput rRNA analysis. *Nucleic Acids Res* 42:D633–42.
- 1377 77. Team RC. 2017. R Core Team (2017). R: A language and environment for statistical
1378 computing. R Found Stat Comput Vienna, Austria URL [http://www R-project org/](http://www.R-project.org/) , page R
1379 Foundation for Statistical Computing.
- 1380 78. McMurdie PJ, Holmes S. 2013. phyloseq: An R Package for Reproducible Interactive
1381 Analysis and Graphics of Microbiome Census Data. *PLoS One* 8:e61217.
- 1382 79. Camacho C, Coulouris G, Avagyan V, Ma N, Papadopoulos J, Bealer K, Madden TL. 2009.
1383 BLAST+: architecture and applications. *BMC Bioinformatics* 10:421.
- 1384 80. Edgar RC. 2004. MUSCLE: multiple sequence alignment with high accuracy and high

- 1385 throughput. *Nucleic Acids Res* 32:1792–1797.
- 1386 81. Capella-Gutiérrez S, Silla-Martínez JM, Gabaldón T. 2009. trimAl: a tool for automated
1387 alignment trimming in large-scale phylogenetic analyses. *Bioinformatics* 25:1972–1973.
- 1388 82. Nguyen L-T, Schmidt HA, von Haeseler A, Minh BQ. 2015. IQ-TREE: a fast and effective
1389 stochastic algorithm for estimating maximum-likelihood phylogenies. *Mol Biol Evol*
1390 32:268–274.
- 1391 83. Hoang DT, Chernomor O, von Haeseler A, Minh BQ, Vinh LS. 2018. UFBoot2: Improving
1392 the Ultrafast Bootstrap Approximation. *Mol Biol Evol* 35:518–522.
- 1393 84. Junier T, Zdobnov EM. 2010. The Newick utilities: high-throughput phylogenetic tree
1394 processing in the UNIX shell. *Bioinformatics* 26:1669–1670.
- 1395 85. Han MV, Zmasek CM. 2009. phyloXML: XML for evolutionary biology and comparative
1396 genomics. *BMC Bioinformatics* 10:356.
- 1397 86. Stingl U, Cho JC, Foo W, Vergin KL, Lanoil B, Giovannoni SJ. 2008. Dilution-to-
1398 extinction culturing of psychrotolerant planktonic bacteria from permanently ice-covered
1399 lakes in the McMurdo Dry Valleys, Antarctica. *Microb Ecol* 55:395–405.
- 1400 87. Page KA, Connon SA, Giovannoni SJ. 2004. Representative freshwater bacterioplankton
1401 isolated from Crater Lake, Oregon. *Appl Environ Microbiol* 70:6542–6550.
- 1402 88. Noell SE, Giovannoni SJ. 2019. SAR11 bacteria have a high affinity and multifunctional
1403 glycine betaine transporter. *Environ Microbiol* 21:2559–2575.
- 1404 89. Thume K, Gebser B, Chen L, Meyer N, Kieber DJ, Pohnert G. 2018. The metabolite
1405 dimethylsulfoxonium propionate extends the marine organosulfur cycle. *Nature* 563:412–
1406 415.
- 1407 90. Asher EC, Dacey JWH, Stukel M, Long MC, Tortell PD. 2017. Processes driving seasonal
1408 variability in DMS, DMSP, and DMSO concentrations and turnover in coastal Antarctic
1409 waters. *Limnol Oceanogr* 62:104–124.
- 1410 91. Mizuno CM, Rodriguez-Valera F, Ghai R. 2015. Genomes of planktonic Acidimicrobiales:
1411 widening horizons for marine Actinobacteria by metagenomics. *MBio* 6:e02083–14.
- 1412 92. Lee J, Kwon KK, Lim S-I, Song J, Choi AR, Yang S-H, Jung K-H, Lee J-H, Kang SG, Oh
1413 H-M, Cho JC. 2019. Isolation, cultivation, and genome analysis of proteorhodopsin-
1414 containing SAR116-clade strain *Candidatus Puniceispirillum marinum* IMCC1322. *J*
1415 *Microbiol* 57:676–687.
- 1416 93. Kitzinger K, Padilla CC, Marchant HK, Hach PF, Herbold CW, Kidane AT, Könneke M,
1417 Littmann S, Mooshammer M, Niggemann J, Petrov S, Richter A, Stewart FJ, Wagner M,
1418 Kuypers MMM, Bristow LA. 2019. Cyanate and urea are substrates for nitrification by
1419 Thaumarchaeota in the marine environment. *Nat Microbiol* 4:234–243.

- 1420 94. Kamennaya NA, Post AF. 2011. Characterization of cyanate metabolism in marine
1421 *Synechococcus* and *Prochlorococcus* spp. *Appl Environ Microbiol* 77:291–301.
- 1422 95. Eren AM, Maignien L, Sul WJ, Murphy LG, Grim SL, Morrison HG, Sogin ML. 2013.
1423 Oligotyping: Differentiating between closely related microbial taxa using 16S rRNA gene
1424 data. *Methods Ecol Evol* 4:1111–1119.
- 1425 96. Needham DM, Fuhrman JA. 2016. Pronounced daily succession of phytoplankton, archaea
1426 and bacteria following a spring bloom. *Nat Microbiol* 1:16005.
- 1427 97. Campbell BJ, Yu L, Heidelberg JF, Kirchman DL. 2011. Activity of abundant and rare
1428 bacteria in a coastal ocean. *Proc Natl Acad Sci U S A* 108:12776–12781.
- 1429 98. Oh HM, Kwon KK, Kang I, Kang SG, Lee JH, Kim SJ, Cho JC. 2010. Complete genome
1430 sequence of “*Candidatus puniceispirillum marinum*” IMCC1322, a representative of the
1431 SAR116 clade in the Alphaproteobacteria. *J Bacteriol* 192:3240–3241.
- 1432 99. Fegatella F, Lim J, Kjelleberg S, Cavicchioli R. 1998. Implications of rRNA operon copy
1433 number and ribosome content in the marine oligotrophic ultramicrobacterium
1434 *Sphingomonas* sp. strain RB2256. *Appl Environ Microbiol* 64:4433–4438.
- 1435 100. Acinas SG, Marcelino LA, Klepac-Ceraj V, Polz MF. 2004. Divergence and redundancy
1436 of 16S rRNA sequences in genomes with multiple *rrn* operons. *J Bacteriol* 186:2629–2635.
- 1437 101. Pedrós-Alió C. 2012. The rare bacterial biosphere. *Ann Rev Mar Sci* 4:449–466.
- 1438 102. Martiny AC. 2019. High proportions of bacteria are culturable across major biomes.
1439 *ISME J* 13:2125–2128.
- 1440 103. Parada AE, Needham DM, Fuhrman JA. 2015. Every base matters: assessing small
1441 subunit rRNA primers for marine microbiomes with mock communities, time series and
1442 global field samples. *Environ Microbiol* 18:1403–1414.
- 1443 104. Del Giorgio PA, Gasol JM. 2008. Physiological structure and single-cell activity in
1444 marine bacterioplankton. *Microbial Ecology of the Oceans* 2:243–298.
- 1445 105. Malmstrom RR, Kiene RP, Cottrell MT, Kirchman DL. 2004. Contribution of SAR11
1446 bacteria to dissolved dimethylsulfoniopropionate and amino acid uptake in the North
1447 Atlantic Ocean. *Appl Environ Microbiol* 70:4129–4135.
- 1448 106. Malmstrom RR, Cottrell MT, Elifantz H, Kirchman DL. 2005. Biomass production and
1449 assimilation of dissolved organic matter by SAR11 bacteria in the Northwest Atlantic
1450 Ocean. *Appl Environ Microbiol* 71:2979–2986.
- 1451 107. Piwosz K, Salcher MM, Zeder M, Ameryk A, Pernthaler J. 2013. Seasonal dynamics and
1452 activity of typical freshwater bacteria in brackish waters of the Gulf of Gdańsk. *Limnol*
1453 *Oceanogr* 58:817–826.

- 1454 108. Laghdass M, Catala P, Caparros J, Oriol L, Lebaron P, Obernosterer I. 2012. High
1455 contribution of SAR11 to microbial activity in the north west Mediterranean Sea. *Microb*
1456 *Ecol* 63:324–333.
- 1457 109. Salter I, Galand PE, Fagervold SK, Lebaron P, Obernosterer I, Oliver MJ, Suzuki MT,
1458 Tricoire C. 2015. Seasonal dynamics of active SAR11 ecotypes in the oligotrophic
1459 Northwest Mediterranean Sea. *ISME J* 9:347–360.
- 1460 110. Leizeaga A, Estrany M, Forn I, Sebastián M. 2017. Using Click-Chemistry for
1461 Visualizing in Situ Changes of Translational Activity in Planktonic Marine Bacteria. *Front*
1462 *Microbiol* 8:2360.
- 1463 111. Kirchman DL. 2016. Growth Rates of Microbes in the Oceans. *Ann Rev Mar Sci* 8:285–
1464 309.
- 1465 112. Samo TJ, Smriga S, Malfatti F, Sherwood BP, Azam F. 2014. Broad distribution and high
1466 proportion of protein synthesis active marine bacteria revealed by click chemistry at the
1467 single cell level. *Frontiers in Marine Science* 1:48.
- 1468 113. Smriga S, Samo TJ, Malfatti F, Villareal J, Azam F. 2014. Individual cell DNA synthesis
1469 within natural marine bacterial assemblages as detected by “click”chemistry. *Aquat Microb*
1470 *Ecol* 72:269–280.
- 1471 114. Bradley JA, Amend JP, LaRowe DE. 2019. Survival of the fewest: Microbial dormancy
1472 and maintenance in marine sediments through deep time. *Geobiology* 17:43–59.
- 1473 115. Zhao Y, Temperton B, Thrash JC, Schwalbach MS, Vergin KL, Landry ZC, Ellisman M,
1474 Deerinck T, Sullivan MB, Giovannoni SJ. 2013. Abundant SAR11 viruses in the ocean.
1475 *Nature* 494:357–360.
- 1476 116. Martinez-Hernandez F, Fornas Ò, Lluesma Gomez M, Garcia-Heredia I, Maestre-
1477 Carballa L, López-Pérez M, Haro-Moreno JM, Rodriguez-Valera F, Martinez-Garcia M.
1478 2018. Single-cell genomics uncover Pelagibacter as the putative host of the extremely
1479 abundant uncultured 37-F6 viral population in the ocean. *ISME J* 13:232–236.
- 1480 117. Chen L-X, Zhao Y, McMahon KD, Mori JF, Jessen GL, Nelson TC, Warren LA,
1481 Banfield JF. 2019. Wide Distribution of Phage That Infect Freshwater SAR11 Bacteria.
1482 *mSystems* 4:e00410–19.
- 1483 118. Thingstad TF, Lignell R. 1997. Theoretical models for the control of bacterial growth
1484 rate, abundance, diversity and carbon demand. *Aquat Microb Ecol* 13:19–27.
- 1485 119. Våge S, Storesund JE, Thingstad TF. 2013. SAR11 viruses and defensive host strains.
1486 *Nature* 499:E3–4.
- 1487 120. Thingstad TF, Vage S, Storesund JE, Sandaa RA, Giske J. 2014. A theoretical analysis of
1488 how strain-specific viruses can control microbial species diversity. *Proc Natl Acad Sci U S*
1489 *A* 111:7813–7818.

- 1490 121. Giovannoni S, Temperton B, Zhao Y. 2013. Giovannoni et al. reply. *Nature* 499:E4–E5.
- 1491 122. Alonso-Sáez L, Morán XAG, Clokie MR. 2018. Low activity of lytic pelagiphages in
1492 coastal marine waters. *ISME J* 12:2100–2102.
- 1493 123. Chapman-McQuiston E, Wu XL. 2008. Stochastic receptor expression allows sensitive
1494 bacteria to evade phage attack. Part I: experiments. *Biophys J* 94:4525–4536.
- 1495 124. Bertozzi Silva J, Storms Z, Sauvageau D. 2016. Host receptors for bacteriophage
1496 adsorption. *FEMS Microbiol Lett* 363:fnw002.
- 1497 125. Oliver JD. 2005. The viable but nonculturable state in bacteria. *J Microbiol* 43 Spec
1498 No:93–100.
- 1499 126. Dubnau D, Losick R. 2006. Bistability in bacteria. *Mol Microbiol* 61:564–572.
- 1500 127. Shkoporov AN, Khokhlova EV, Fitzgerald CB, Stockdale SR, Draper LA, Ross RP, Hill
1501 C. 2018. Φ CrAss001 represents the most abundant bacteriophage family in the human gut
1502 and infects *Bacteroides intestinalis*. *Nat Commun* 9:4781.
- 1503 128. Teira E, Martínez-García S, Lønborg C, Alvarez-Salgado XA. 2009. Growth rates of
1504 different phylogenetic bacterioplankton groups in a coastal upwelling system. *Environ*
1505 *Microbiol Rep* 1:545–554.
- 1506 129. Lankiewicz TS, Cottrell MT, Kirchman DL. 2016. Growth rates and rRNA content of
1507 four marine bacteria in pure cultures and in the Delaware estuary. *ISME J* 10:823–832.
- 1508 130. Ferrera I, Gasol JM, Sebastián M, Hojerová E, Koblížek M. 2011. Comparison of growth
1509 rates of aerobic anoxygenic phototrophic bacteria and other bacterioplankton groups in
1510 coastal Mediterranean waters. *Appl Environ Microbiol* 77:7451–7458.
- 1511 131. Carini P, Campbell EO, Morré J, Sañudo-Wilhelmy SA, Thrash JC, Bennett SE,
1512 Temperton B, Begley T, Giovannoni SJ. 2014. Discovery of a SAR11 growth requirement
1513 for thiamin’s pyrimidine precursor and its distribution in the Sargasso Sea. *ISME J* 8:1727–
1514 1738.
- 1515 132. Grant SR, Church MJ, Ferrón S, Laws EA, Rappé MS. 2019. Elemental Composition,
1516 Phosphorous Uptake, and Characteristics of Growth of a SAR11 Strain in Batch and
1517 Continuous Culture. *mSystems* 4:e00218–18.
- 1518 133. White AE, Giovannoni SJ, Zhao Y, Vergin K, Carlson CA. 2019. Elemental content and
1519 stoichiometry of SAR11 chemoheterotrophic marine bacteria. *Limnology and*
1520 *Oceanography Letters* 4:44–51.
- 1521 134. Smith DP, Cameron Thrash J, Nicora CD, Lipton MS, Burnum-Johnson KE, Carini P,
1522 Smith RD, Giovannoni SJ. 2013. Proteomic and Transcriptomic Analyses of “*Candidatus*
1523 *Pelagibacter ubique*” Describe the First PII-Independent Response to Nitrogen Limitation in
1524 a Free-Living Alphaproteobacterium. *MBio* 4:e00133–12.

1525 135. van Vliet S, Dal Co A, Winkler AR, Spriewald S, Stecher B, Ackermann M. 2018.
1526 Spatially Correlated Gene Expression in Bacterial Groups: The Role of Lineage History,
1527 Spatial Gradients, and Cell-Cell Interactions. *Cell Syst* 6:496–507.e6.

1528

Figure S1

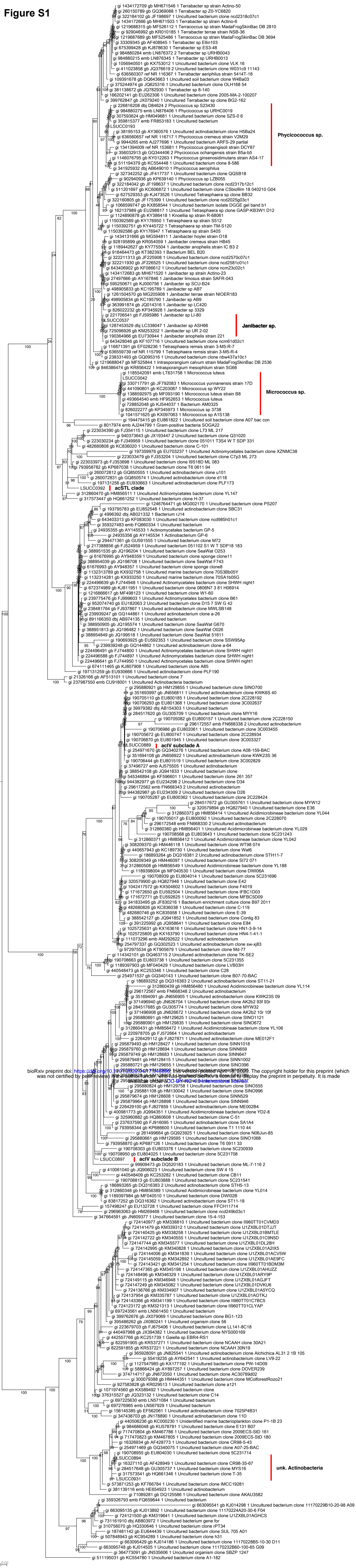
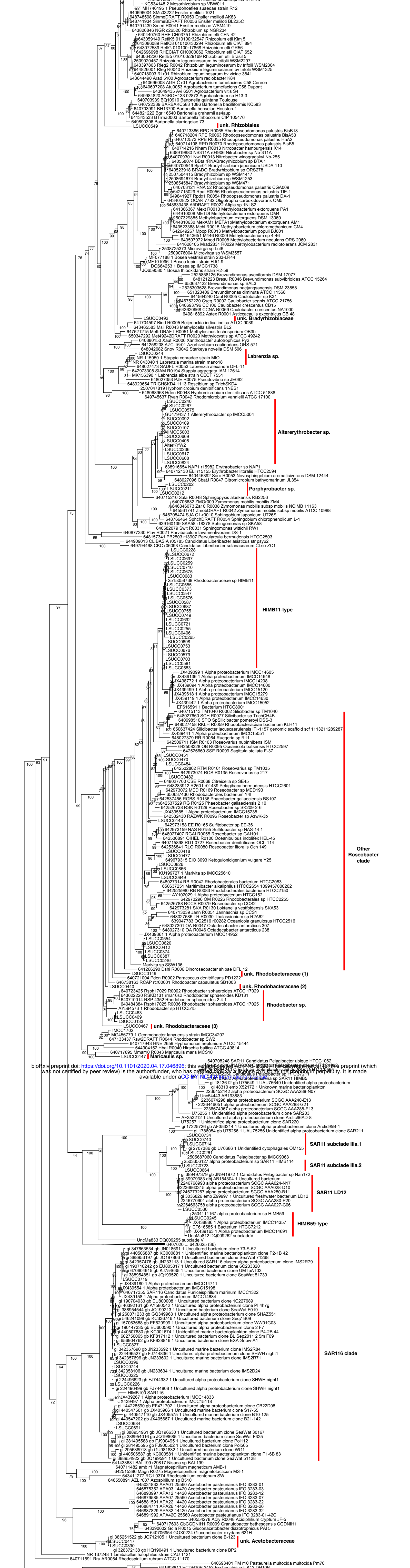
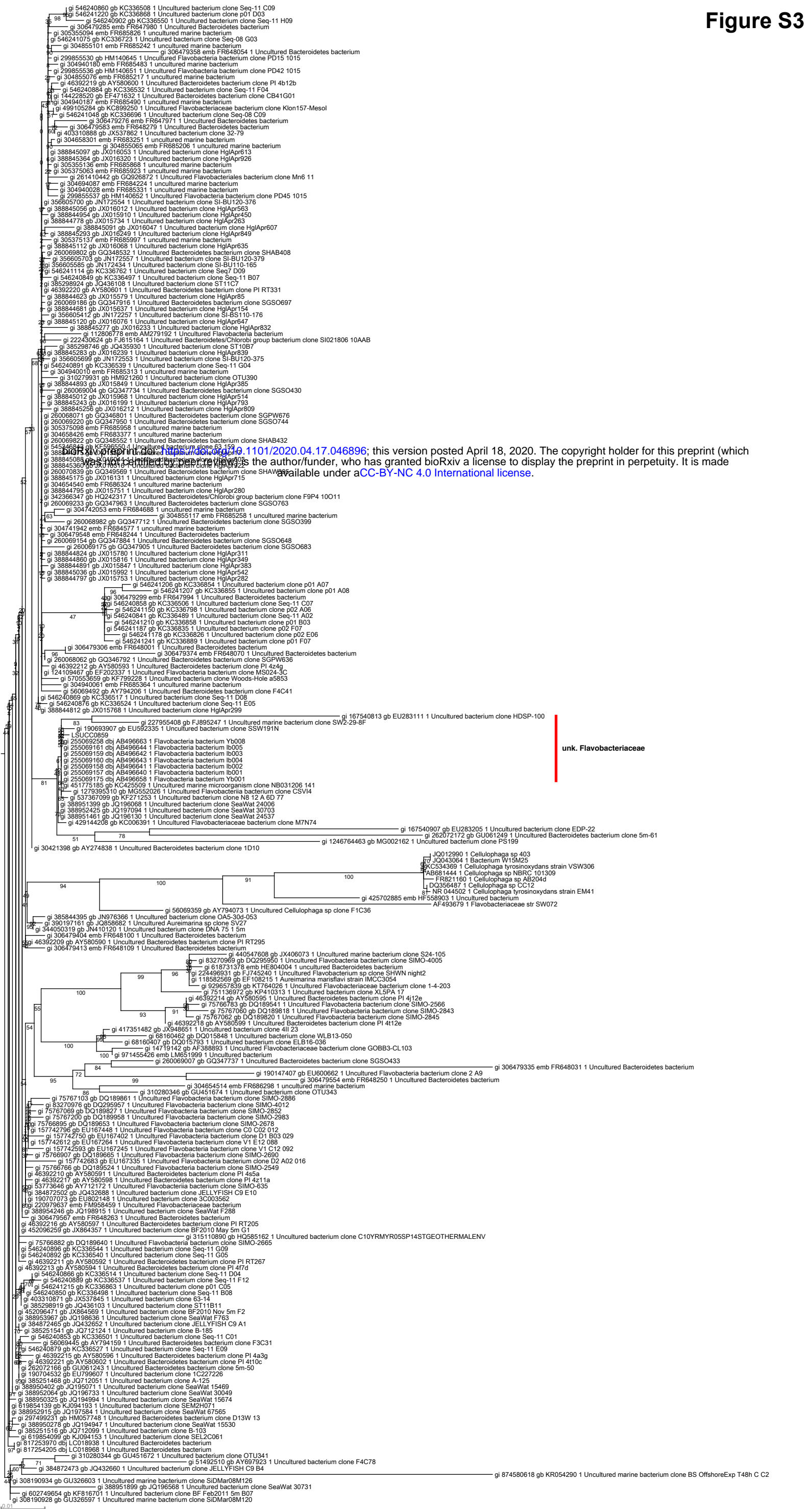


Figure S2



bioRxiv preprint doi: <https://doi.org/10.1101/2020.04.17.046896>; this version posted April 16, 2020. The copyright holder for this preprint (which was not certified by peer review) is the author/funder, who has granted bioRxiv a license to display the preprint in perpetuity. It is made available under aCC-BY-NC 4.0 International license.



bioRxiv preprint doi: <https://doi.org/10.1101/2020.04.17.046896>; this version posted April 18, 2020. The copyright holder for this preprint (which was not certified by peer review) is the author/funder, who has granted bioRxiv a license to display the preprint in perpetuity. It is made available under [aCC-BY-NC 4.0 International license](https://creativecommons.org/licenses/by-nc/4.0/).

unk. Flavobacteriaceae

Cellulophaga sp. clade 100

0.01

0.01

Figure S4

